
ON THE RELATIONSHIP BETWEEN CONTINUAL LEARNING AND LONG-TAILED RECOGNITION

Mahdiyari Molahasani, Michael Greenspan, Ali Etemad

Department of Electrical and Computer Engineering & Ingenuity Labs Research Institute
Queen’s University
Kingston, Canada

{m.molahasani, michael.greenspan, ali.etemad}@queensu.ca

ABSTRACT

Real-world datasets often exhibit long-tailed distributions, where a few dominant “Head” classes have abundant samples while most “Tail” classes are severely underrepresented, leading to biased learning and poor generalization for the Tail. We present a theoretical framework that reveals a previously undescribed connection between Long-Tailed Recognition (LTR) and Continual Learning (CL), the process of learning sequential tasks without forgetting prior knowledge. Our analysis demonstrates that, for models trained on imbalanced datasets, the weights converge to a bounded neighborhood of those trained exclusively on the Head, with the bound scaling as the inverse square root of the imbalance factor. Leveraging this insight, we introduce Continual Learning for Long-Tailed Recognition (CLTR), a principled approach that employs standard off-the-shelf CL methods to address LTR problems by sequentially learning Head and Tail classes without forgetting the Head. Our theoretical analysis further suggests that CLTR mitigates gradient saturation and improves Tail learning while maintaining strong Head performance. Extensive experiments on CIFAR100-LT, CIFAR10-LT, ImageNet-LT, and Caltech256 validate our theoretical predictions, achieving strong results across various LTR benchmarks. Our work bridges the gap between LTR and CL, providing a principled way to tackle imbalanced data challenges with standard existing CL strategies.

1 Introduction

Real-world data often exhibits long-tailed distributions [1, 2, 3, 4], where a small set of “Head” classes dominates with abundant samples, while the vast majority of “Tail” classes are severely underrepresented. This imbalance poses a fundamental challenge for deep learning: the Head classes disproportionately influence gradients during training, causing models to converge toward solutions that favor the Head while failing to generalize to the Tail [5, 6, 7].

To address this issue, various methods have been proposed, including sample-wise balancing through over-sampling the Tail classes [8, 9, 10], transfer learning approaches to adapt knowledge from Head to Tail [11, 12, 13, 14], loss- or gradient-wise balancing to mitigate class size effects [15, 16, 17], and weight regularization for ensuring balanced weight magnitudes during training [5]. More recently, *multi-stage training* has emerged as a promising solution for reducing sensitivity to Tail variations and model variance [18, 19]. Concurrently, Continual Learning (CL) has evolved as a paradigm to learn sequences of tasks without forgetting previously acquired knowledge [20]. The structural similarity between multi-stage Long-Tailed Recognition (LTR) and sequential learning prompts a fundamental question:

Can solution approaches to continual learning be harnessed to solve long-tailed recognition?

To answer this, we first establish a theoretical foundation for model convergence under imbalance. We prove that training on a long-tailed dataset yields weights analytically close to those obtained by training *exclusively* on Head classes, with a bound scaling as $\mathcal{O}(1/\sqrt{\text{IF}})$ (Fig. 1 left). This insight suggests a natural progression for addressing LTR: sequentially learning the Head first, followed by the Tail while preserving Head information. By preserving Head knowledge while accommodating the Tail, we uncover a strong duality between LTR and CL, implying that off-the-shelf CL methods can be effectively repurposed for LTR.

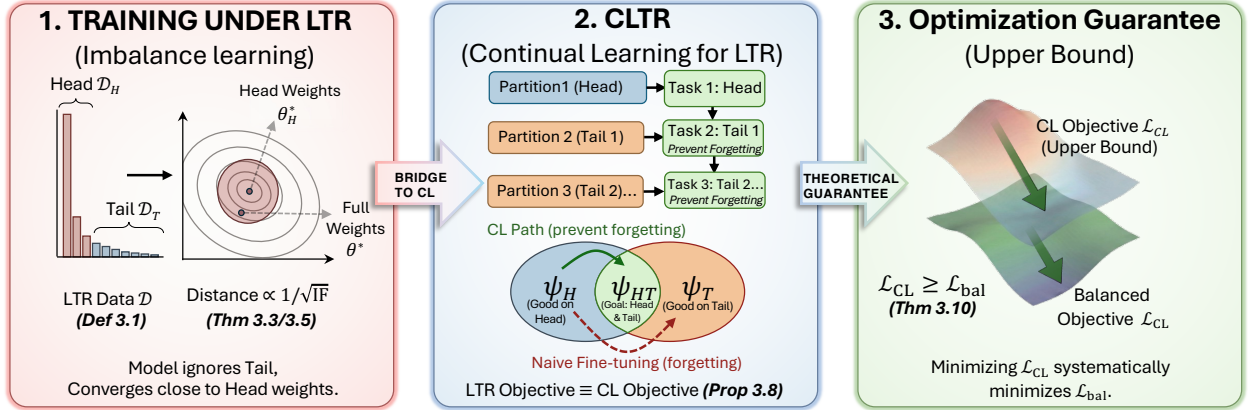


Figure 1: Overview of our framework: (left) theoretical analysis of convergence under the LTR setup, showing how imbalance drives convergence toward head-class solutions; (middle) our proposed CLTR reformulating LTR as a CL problem; and (right) optimization guarantee demonstrating that minimizing CL objective provides an upper bound that systematically improves the balanced LTR objective.

Based on this perspective, we introduce Continual Learning for Long-Tailed Recognition (CLTR), a streamlined framework that reformulates LTR as a sequential learning problem. The model first learns the Head, followed by the Tail, leveraging CL techniques to mitigate catastrophic forgetting and ensure balanced learning (Fig. 1 middle). Crucially, we provide a theoretical guarantee that the CL objective serves as an upper bound of the balanced LTR objective, ensuring systematic performance improvements (Fig. 1 right).

We validate the efficacy of CLTR through extensive experiments on five datasets: MNIST-LT, CIFAR100-LT, CIFAR10-LT, ImageNet-LT, and Caltech256. First, we use the MNIST-LT and CIFAR100-LT datasets to empirically verify our theoretical predictions about weight dynamics during Head-only and full-dataset (long-tailed) training. Next, we evaluate the performance of CLTR across commonly used LTR benchmarks (CIFAR100-LT, CIFAR10-LT, and ImageNet-LT) under varying imbalance factors, consistently achieving strong results. To demonstrate the effectiveness of our proposed framework on more challenging LTR scenarios, we benchmark CLTR against recent approaches for Long-Tail Class-Incremental Learning (LT-CIL). These experiments demonstrate the strong performance of our framework in addressing both LTR and LT-CIL challenges. Our contributions are summarized as follows:

1. **Theoretical Analysis of Convergence:** We prove upper bounds on the distance between parameters learned on imbalanced partitions, showing this distance scales inversely with the square root of the imbalance factor, $\mathcal{O}(1/\sqrt{\text{IF}})$ (Theorems 3.3 and 3.5).
2. **Reformulating LTR as CL:** We uncover a previously unrevealed connection between the two fields, formally proposing that Long-Tailed Recognition is structurally equivalent to a Continual Learning problem (Proposition 3.8), thereby repurposing CL methods for imbalanced learning.
3. **The CLTR Framework:** Building on this reformulation, we introduce CLTR, a streamlined framework that learns Head and Tail classes sequentially using standard CL techniques to mitigate catastrophic forgetting (Algorithm A1).
4. **Optimization Guarantee:** We provide a theoretical proof that minimizing the standard CL objective constitutes optimizing an upper bound of the balanced LTR objective (Theorem 3.10), ensuring that CLTR systematically improves balanced performance.
5. **Empirical Validation:** We demonstrate that CLTR achieves strong performance across standard LTR benchmarks and effectively handles complex LT-CIL scenarios.

By providing a principled framework and bridging the fields of LTR and CL, this work sheds light on the underlying mechanisms of LTR and opens new avenues for leveraging advancements in CL to address real-world challenges of imbalanced data.

2 Related Work

Long-Tailed Recognition. LTR methods broadly fall into: (i) *data distribution re-balancing*, (ii) *class-balanced losses*, and (iii) *Head-to-Tail transfer learning* [21]. Re-balancing includes Tail over-sampling [8, 22], Head under-sampling

[23], class-balanced sampling [24, 25], and dynamic label distribution shift [26]. Class-balanced losses reweight samples using class statistics [15, 16, 27], focal loss [28], or Bayesian uncertainty [29]. Transfer learning leverages Head features to improve Tail performance [30, 11, 31]. Recently, multi-stage Head/Tail training has emerged as an effective LTR strategy: BBN improves representation learning [18], while RIDE reduces model variance via diverse experts [32]. These methods implicitly adopt sequential training, but rely on heuristic LTR-specific architectures. In contrast, we provide a theoretical unification explaining *why* sequential methods work: we show such specialized methods are subsets of a broader phenomenon, and by framing LTR as a CL problem, we enable *any* off-the-shelf CL algorithm to address LTR without complex, LTR-specific architectural modifications. This also allows us to leverage a rich CL literature that, unlike existing multi-stage LTR solutions, tends to use a single network throughout training.

Although many works study LTR empirically, very few approach it theoretically [33, 34]. These works show the Head is learned faster than the Tail, focusing on training dynamics; in contrast, our theory studies the *convergence point* in LTR and unifies *why* sequential strategies work, establishing that specialized LTR methods are subsets of this broader phenomenon.

Continual Learning. CL methods are commonly categorized as *expansion-based*, *regularization-based*, and *memory-based*. Expansion-based methods allocate task-specific parameters [35, 36, 37], but can grow unbounded as tasks accumulate; FOSTER mitigates this with a two-stage expand-then-compress paradigm [38]. Regularization-based methods constrain changes to important parameters via loss penalties [39, 40, 41, 42, 20]. Memory-based approaches use replay buffers to reduce forgetting [43, 44, 45]. For class-incremental learning without test-time task IDs, TPL predicts task IDs via likelihood ratios using replay data and task-specific models within a shared network [46]. More recently, gradient surgery projects new-task gradients onto directions orthogonal to previous tasks to limit interference [39, 47], achieving state-of-the-art CL performance.

3 Proposed Approach

3.1 Training on Long-Tailed Distributions

Here, we first define the LTR problem and then analyze the behavior of a model when trained under LTR setup to provide a theoretical basis for our proposed CLTR framework. For the summary of the notations see Appendix A.

Let’s consider the input space to be \mathbb{R}^d , where each input is represented by \mathbf{x}_i , and the label space is $\{1, \dots, k\}$, where each label is denoted by y_i . Let \mathcal{D} denote the training set containing samples (\mathbf{x}_i, y_i) . \mathcal{D}_c is a set of all samples belonging to class c denoted as $\mathcal{D}_c = \{(\mathbf{x}_i, y_i) \in \mathcal{D} \mid y_i = c\}$ and $|\mathcal{D}_c|$ represents its cardinality. Without loss of generality, let the classes be ordered by their cardinalities such that $|\mathcal{D}_i| \geq |\mathcal{D}_j|$ for all $i < j$. Following [48], let \mathcal{D}_H and \mathcal{D}_T represent the subsets of \mathcal{D} corresponding to the Head set and Tail set, respectively as $\mathcal{D}_H = \{(\mathbf{x}_i, y_i) \in \mathcal{D} : y_i \leq c_k\}$ and $\mathcal{D}_T = \{(\mathbf{x}_i, y_i) \in \mathcal{D} : y_i > c_k\}$, where c_k denotes the number of classes in the Head set. As a result, every class in the Head has more samples than any class in the Tail. The loss function over \mathcal{D}_c is defined as $\mathcal{L}(\mathcal{D}_c, \theta) = \frac{1}{|\mathcal{D}_c|} \sum_{i=1}^{|\mathcal{D}_c|} \ell((\mathbf{x}_i, y_i), \theta)$, where $(\mathbf{x}_i, y_i) \in \mathcal{D}_c$. Note that $\ell((\mathbf{x}_i, y_i), \theta)$ is the loss of each individual sample. For brevity, we will henceforth use notations $\mathcal{L}_{\mathcal{D}_c} = \mathcal{L}_{\mathcal{D}_c}(\theta) = \mathcal{L}(\mathcal{D}_c, \theta)$ and $\ell((\mathbf{x}_i, y_i)) = \ell_{(\mathbf{x}_i, y_i)}(\theta) = \ell((\mathbf{x}_i, y_i), \theta)$.

LTR aims to address the challenge of learning from highly imbalanced data. This occurs when the training data \mathcal{D} contains more samples in Head set (\mathcal{D}_H) and fewer in the Tail set (\mathcal{D}_T). The imbalance factor IF quantifies the severity of this issue in a dataset, defined as:

$$\text{IF} = \frac{|\mathcal{D}_{c^{\max}}|}{|\mathcal{D}_{c^{\min}}|}, \quad (1)$$

where $c^{\max} = \arg \max_c |\mathcal{D}_c|$, and $c^{\min} = \arg \min_c |\mathcal{D}_c|$, such that $\mathcal{D}_{c^{\max}} \in \mathcal{D}_H$ and $\mathcal{D}_{c^{\min}} \in \mathcal{D}_T$. Now we formally define a long-tailed dataset and the LTR problem:

Definition 3.1. A dataset is deemed *long-tailed* when $|\mathcal{D}_{c^{\max}}| \gg |\mathcal{D}_{c^{\min}}|$ or, in other words, $\text{IF} \gg 1$. When a model is trained on such a dataset and its performance is assessed on a test set where each class c has the same number of samples (i.e. $|\mathcal{D}_c| = \kappa$ for each class c within the test set where κ is a constant number), the problem is referred to as *Long-Tailed Recognition*.

3.2 Convex Case: Baseline Analysis

Here we address the case that the loss function is convex (as illustrated in Fig. 2 left), as detailed in the following:

Assumption 3.2. Let the size of all Head classes be equal, and the size of all Tail classes be equal, i.e. $|\mathcal{D}_i| = |\mathcal{D}_j|$ for all $\mathcal{D}_i, \mathcal{D}_j \in \mathcal{D}_H$ and $|\mathcal{D}_k| = |\mathcal{D}_l|$ for all $\mathcal{D}_k, \mathcal{D}_l \in \mathcal{D}_T$ (this condition will be relaxed in Assumption 3.6). Also, let the

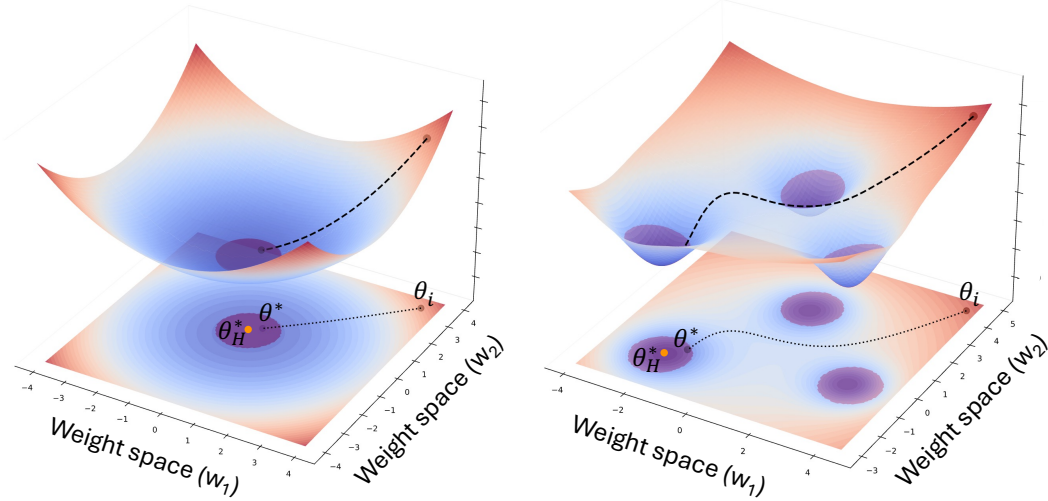


Figure 2: Illustration of the Head loss landscape (\mathcal{L}_H). Left: convex setting (Assumption 3.2); the unique minimizer (θ_H^*) is marked in orange. Right: Feedforward deep network, $\text{KL}(1/2)$ setting (Assumption 3.4); multiple local minimizers ($\theta_{H,k}^*$) are shown in orange. In both panels, the red region denotes the provable neighborhood that contains the parameter (θ^*) obtained when training on the full long-tailed dataset; its radius scales as $\mathcal{O}(1/\sqrt{\text{IF}})$ by Theorems 3.3 and 3.5. (Top: surface; bottom: contour projection.)

model be a classifier with parameters θ trained with a convex loss function \mathcal{L} , with an additional L^2 regularization term utilized in the training to prevent the weights from growing excessively.

We now introduce Theorem 3.3 demonstrating the relationship between the weights of the model when it is trained solely on the Head as well as on the entire dataset.

Theorem 3.3. *Given Assumption 3.2, if a model is trained in an LTR setting (Definition 3.1), then the weights of the model after training (θ^*) will lie within the bounded neighborhood of the model’s weight if solely trained on Head (θ_H^*), with the scale of:*

$$\|\theta^* - \theta_H^*\| = \mathcal{O}\left(\frac{1}{\sqrt{\text{IF}}}\right). \quad (2)$$

Proof Sketch. For the full proof see Appendix B.1. We start by expressing the total loss as a weighted combination of the Head and Tail set losses, where the weights depend on the dataset imbalance factor IF . As IF becomes larger, the contribution of the Tail set loss diminishes, and the total loss approaches the Head set loss. Next, we bound the difference between the total loss and the Head set loss in terms of IF . Using a lemma that connects loss differences to the proximity of their respective minimizers under Assumption 3.2, we translate this bound into a relationship between the model parameters obtained from the total dataset and those obtained from the Head set. Finally, we show that the loss difference scales as $\mathcal{O}(1/\text{IF})$, leading to the parameter difference scaling of $\mathcal{O}(1/\sqrt{\text{IF}})$.

3.3 Extension to Feedforward Deep Networks

Assumption 3.2 posits a convex loss with L^2 regularization, which is convenient for analysis but not representative of modern deep networks, whose training losses are typically nonconvex. We now relax convexity and work under the widely used *Kurdyka–Łojasiewicz* (KL) framework, together with a local geometric condition that is standard for deep nets near minimizers [49] (Fig. 2 right).

Assumption 3.4. The model is a feedforward deep neural network with piecewise-analytic/definable activations (e.g., ReLU/LeakyReLU/softplus) and a standard empirical loss (e.g., cross-entropy or squared loss). Hence the loss \mathcal{L} enjoys the *Kurdyka–Łojasiewicz* (KL) property with exponent $1/2$ in a neighborhood of S_H (which represents the set of minima of \mathcal{L}) [50].

Under this relaxed assumption we obtain the same scaling as in the convex case:

Theorem 3.5. *Given Assumption 3.4, there exists a bound for the distance between the weights of the model after training (θ^*) and one of the minima of the loss when training on the head solely, scaling inversely with the square root of the imbalance factor:*

$$\text{dist}(\theta^*, S_H) = \mathcal{O}\left(\frac{1}{\sqrt{\text{IF}}}\right). \quad (3)$$

Proof Sketch. For the full proof see Appendix B.3. The proof first establishes a Hölder–1/2 error bound based on the loss’s KL property and piecewise strong convexity (Assumption 3.4), which links the parameter distance $\text{dist}(\theta^*, S_H)$ to the square root of the Head-set loss difference. To bound this loss difference in terms of IF, we decompose it by adding and subtracting the total loss \mathcal{L} at the optimal points θ^* and θ_H^* . Using the optimality of θ^* for \mathcal{L} , we simplify the inequality by removing a non-positive term. Finally, we apply the bound from Eq. 22, which limits the deviation between \mathcal{L} and \mathcal{L}_H to $\mathcal{O}(1/\text{IF})$, to the remaining terms. This shows the loss difference $\mathcal{L}_H(\theta^*) - \mathcal{L}_H(\theta_H^*)$ scales as $\mathcal{O}(1/\text{IF})$, and substituting this back into the Hölder bound (Eq. 40) gives the final parameter distance scaling of $\mathcal{O}(1/\sqrt{\text{IF}})$.

3.4 Extension to Multiple Head–Tail Partitions

Theorems 3.3 and 3.5 assume that there is only one Head and one Tail in the dataset, which is not the case in many real-world datasets. We relax our assumption regarding the data as follows:

Assumption 3.6. We relax Assumptions 3.2 and 3.4 by allowing individual classes within the respective Head or Tail sets to vary in size.

Under the relaxed assumption where the size of the classes within Head and Tail sets differ, these sets can be further partitioned into their own distinct Head and Tail subsets. While each individual partition remains imbalanced, we continue to subdivide them until: (1) $|\mathcal{D}^i| \gg |\mathcal{D}^j|$ for $i < j$, and (2) $\text{IF}_{\mathcal{D}^i} \gg 1$ for all partitions \mathcal{D}^i . In this scenario, none of the partitions of the dataset are long-tailed. Theorem 3.7 extends Theorems 3.3 and 3.5 to address this scenario for any number of partitions.

Theorem 3.7. *Following Assumption 3.6, when dataset \mathcal{D} is divided into n partitions sorted based on their cardinality, i.e. $|\mathcal{D}^i| > |\mathcal{D}^j|$ for all $i < j$, then, the weights θ^* obtained from training the model on \mathcal{D} will always be in a bounded neighborhood of the weights $\theta_{\mathcal{D}^1}^*$ obtained from training on the largest subset of \mathcal{D} with the scale of:*

$$\begin{aligned} \|\theta_{\mathcal{D}^1}^* - \theta^*\| &= \sum_{i=2}^n \mathcal{O}\left(\sqrt{\frac{|\mathcal{D}^i|}{\sum_{j=1}^{i-1} |\mathcal{D}^j|}}\right) \\ &\approx \mathcal{O}\left(\frac{1}{\sqrt{\text{IF}_{\mathcal{D}^1, \mathcal{D}^2}}}\right), \end{aligned} \quad (4)$$

where $\text{IF}_{\mathcal{D}^1, \mathcal{D}^2} = \frac{|\mathcal{D}^1|}{|\mathcal{D}^2|}$.

Proof Sketch. The formal proof is presented in Appendix B.4. Starting with the largest partition \mathcal{D}^1 , we apply Theorem 3.5 to bound the weight difference between the model trained on \mathcal{D}^1 and the model trained on $\mathcal{D}^1 \cup \mathcal{D}^2$. Next, the aggregated subset $\mathcal{D}^1 \cup \mathcal{D}^2$ is treated as the new ‘largest’ subset, and Theorem 3.5 is applied again to bound the weight difference with $\mathcal{D}^1 \cup \mathcal{D}^2 \cup \mathcal{D}^3$. This process is repeated for all partitions, sequentially aggregating subsets and bounding their contributions to the total weight difference. The triangle inequality is then used to combine these bounds into a cumulative upper bound for the total weight difference between the model trained on the largest partition \mathcal{D}^1 and the model trained on the full dataset \mathcal{D} .

3.5 Continual Learning for Long-Tailed Recognition

Let us assume an LTR problem and a learner with a set of parameters denoted as θ (recall definition 3.1). Initially, the learner is trained on a highly imbalanced dataset \mathcal{D} , as shown in Fig. 3, where θ_i is the initialized model in the weight space. Owing to the larger number of Head samples in each iteration, they dominate the evolution of the gradients, resulting in a learner that performs significantly better on the Head set than on the Tail set at the end of training. This process leads the parameters to converge to θ^* . We showed in Theorems 3.3 and 3.7 that θ^* lies within a bounded neighborhood of the learner’s weights θ_H^* when trained exclusively on the Head set \mathcal{D}_H , where the bound is inversely

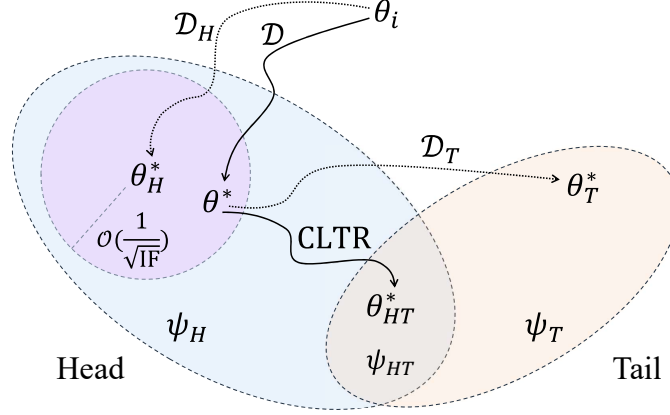


Figure 3: Overview of learning under the LTR scenario and our proposed CLTR approach (symbols described in the text).

proportional to the imbalance factor by the scale of $\mathcal{O}(\frac{1}{\sqrt{\text{IF}}})$. This neighborhood falls in ψ_H which represents an area within the weight space where the network performs well on the Head set. At this stage, the model should learn the Tail; however, if it is simply fine-tuned on the Tail (\mathcal{D}_T), then it results in moving towards θ_T^* in ψ_T and will likely leave ψ_H . This phenomenon occurs in sequential learning and it is known as catastrophic forgetting. To mitigate this problem and guide the model to the intersection of ψ_H and ψ_T denoted as ψ_{HT} , where the model performs well on both Head and Tail, the Tail should be learned without forgetting the Head. To this end, we propose using the standard CL methods for sequentially learning the Tail after the Head while avoiding catastrophic forgetting (converging to θ_{HT}^*).

Following [51], a general CL problem can be formulated as a model exposed to a stream of N incoming training datasets $\mathcal{D}_{\mathcal{Y}_t} = \{(x_i, y_i) | y_i \in \mathcal{Y}_t\}$ for $1 \leq t \leq N$, where \mathcal{Y}_t is the corresponding set of labels. Up to the current timestep t , the set of labels $\bigcup_{i=1}^t \mathcal{Y}_i$ in dataset $\bigcup_{i=1}^t \mathcal{D}_{\mathcal{Y}_i}$ has been previously used in training of the network. The objective at the next timestep $t+1$ is to find a mapping $f_\theta : x \rightarrow y$ that accurately maps sample x to $\bigcup_{i=1}^t \mathcal{Y}_i \cup \mathcal{Y}_{t+1}$, where \mathcal{Y}_{t+1} is the set of new unseen labels in the incoming new dataset $\mathcal{D}_{\mathcal{Y}_{t+1}} = \{(x_i, y_i) | y_i \in \mathcal{Y}_{t+1}\}$. Therefore the ultimate objective of CL is to find an accurate mapping $f_\theta : x \rightarrow y$ for all $(x, y) \in \bigcup_{i=1}^N \mathcal{D}_{\mathcal{Y}_i}$.

Consider dataset \mathcal{D} under the LTR setup (Definition 3.1) divided into N partitions with substantially different sizes sorted based on cardinality such that $\mathcal{D} = \bigcup_{i=1}^N \mathcal{D}^i$ and $|\mathcal{D}^i| \gg |\mathcal{D}^{i+1}|$. We have shown in Theorem 3.3 and Theorem 3.7 that θ^* (the weights of the model when trained on the entire dataset) will be very close to θ_1^* , which is the weights of the model when it is only trained on \mathcal{D}^1 (the largest partition of the dataset). As a result, the model after training on \mathcal{D} can be considered as $f_{\theta_1^*} : x \rightarrow y$ for all $(x, y) \in \mathcal{D}_1$. On the other hand, following Definition 3.1, the objective of LTR is to learn $f_\theta : x \rightarrow y$ for all $(x, y) \in \mathcal{D} = \bigcup_{i=1}^N \mathcal{D}^i$. Hence, additional training steps are required for the model to further learn the rest of the partitions of the dataset ($\bigcup_{i=2}^N \mathcal{D}^i$). Thus, if we consider each of the partitions of the LTR dataset (\mathcal{D}^i for $1 \leq i \leq N$) as an incoming CL dataset ($\mathcal{D}_{\mathcal{Y}_t}$ for $1 \leq t \leq N$), the objective of the LTR problem would be equivalent to the objective of CL. This novel perspective is presented in the following proposition.

Proposition 3.8. *Let dataset \mathcal{D} under the LTR setup (Definition 3.1) be divided into N partitions sorted by cardinality such that $\mathcal{D} = \bigcup_{i=1}^N \mathcal{D}^i$, where $|\mathcal{D}^i| \gg |\mathcal{D}^{i+1}|$. If each partition \mathcal{D}^i is treated as an incoming dataset in a continual learning stream, then the objective of the LTR problem is equivalent to the objective of a CL problem, with the goal of learning:*

$$f_\theta : x \rightarrow y \quad \text{s.t.} \quad (x, y) \in \bigcup_{t=1}^N \mathcal{D}_{\mathcal{Y}_t} \quad (5)$$

$$\mathcal{D}_{\mathcal{Y}_1} = \mathcal{D}^1, \mathcal{D}_{\mathcal{Y}_2} = \mathcal{D}^2, \dots, \mathcal{D}_{\mathcal{Y}_N} = \mathcal{D}^N.$$

A corollary of Proposition 3.8 is that CL solutions can be employed to address LTR. To operationalize this insight, we propose CLTR, a simple yet effective framework that leverages off-the-shelf CL methodologies to solve LTR. Algorithm A1 (in Appendix E) lays out the detailed procedure of our framework. First, the long-tailed dataset is partitioned into multiple subsets, each with a smaller imbalance factor IF than the original dataset, as guaranteed by

Theorem 3.7. Starting with the largest partition, each subsequent partition is treated as a new task and learned using CL while retaining knowledge from the previously learned partitions. This Head-to-Tail ordering ensures that the solution on the first (largest) partition plays the role of the Head solution θ_H^* around which our analysis in Proposition 3.8 and Theorem 3.7 is derived, and is also consistent with standard practice in LTR [18, 19].

3.6 General Guarantees for Effectiveness of CLTR

Here we provide a theoretical *guarantee* for the effectiveness of the proposed CLTR, demonstrating that employing any off-the-shelf CL method can address LTR. To this end, we first employ the unified and general formulation of CL solutions proposed by [52], which covers a wide variety of off-the-shelf CL methods:

$$\begin{aligned} \mathcal{L}_{\text{CL}}(\theta) &:= \mathcal{L}_{\text{task}}(\theta) + \alpha D_{\Phi}(h_{\theta}(\cdot), z) + \beta D_{\Psi}(\theta, \theta_H^*), \\ \alpha, \beta &\geq 0. \end{aligned} \quad (6)$$

where h_{θ} is the model, D_{Φ} and D_{Ψ} are Bregman divergences generated by convex C^1 functions Φ and Ψ , and z is a fixed Head reference (e.g., stored logits/predictions at θ_H^*). In CLTR stage-2, $\mathcal{L}_{\text{task}}(\theta)$ is the Tail loss ($\mathcal{L}_{\text{task}} \equiv \mathcal{L}_T$). The assumptions that we have regarding the CL solution on a neighborhood $\mathcal{N} \subset \mathbb{R}^d$ of θ_H^* are as follows:

Assumption 3.9. (Head smoothness) \mathcal{L}_H is L_H^{sm} -smooth at θ_H^* : for all $\theta \in \mathcal{N}$,

$$\mathcal{L}_H(\theta) \leq \mathcal{L}_H(\theta_H^*) + \frac{L_H^{\text{sm}}}{2} \|\theta - \theta_H^*\|^2, \quad \forall \theta \in \mathcal{N}. \quad (7)$$

(Parameter divergence curvature) $D_{\Psi}(\cdot, \theta_H^*)$ is m_{Ψ} -strongly convex:

$$D_{\Psi}(\theta, \theta_H^*) \geq \frac{m_{\Psi}}{2} \|\theta - \theta_H^*\|^2, \quad \forall \theta \in \mathcal{N}. \quad (8)$$

(Output calibration) There exists $c_{\Phi} > 0$ and a fixed Head target $z = z_H^*$ such that:

$$\mathcal{L}_H(\theta) - \mathcal{L}_H(\theta_H^*) \leq c_{\Phi} D_{\Phi}(h_{\theta}(\cdot), z_H^*), \quad \forall \theta \in \mathcal{N}. \quad (9)$$

Here we explain *why Assumption 3.9 is mild*. (i) Eq. 7 is a standard local smoothness bound; it always holds with some finite L_H^{sm} if \mathcal{L}_H has locally Lipschitz gradient. (ii) Eq. 8 holds for quadratic/EWC-type $\Psi(\theta) = \frac{1}{2}(\theta - \theta_H^*)^{\top} H_H (\theta - \theta_H^*)$ with a damped positive-definite $H_H \succeq m_{\Psi} I$ (standard in practice). It also holds on piecewise strongly convex basins (e.g., deep networks with ReLU + weight decay [50]). (iii) Eq. 9 is the usual distillation calibration (e.g., cross-entropy controlled by KL between predictions).

We now propose the general guarantee for the effectiveness of CLTR through the following theorem.

Theorem 3.10. *Suppose Assumption 3.9 holds on \mathcal{N} . Define the thresholds*

$$\beta_{\min} := \frac{L_H^{\text{sm}}}{2m_{\Psi}}, \quad \alpha_{\min} := \frac{c_{\Phi}}{2},$$

where L_H^{sm} is local smoothness constant of \mathcal{L}_H at θ_H^* , m_{Ψ} is strong-convexity constant of $D_{\Psi}(\cdot, \theta_H^*)$, and c_{Φ} is calibration constant relating \mathcal{L}_H to D_{Φ} . If either $\beta \geq \beta_{\min}$ (Parameter route) or $\alpha \geq \alpha_{\min}$ (Output route), then for any $\theta \in \mathcal{N}$,

$$\mathcal{L}_{\text{bal}}(\theta) \leq \mathcal{L}_{\text{CL}}(\theta) + \frac{1}{2} \mathcal{L}_H(\theta_H^*). \quad (10)$$

In words: if either $\beta \geq \beta_{\min}$ or $\alpha \geq \alpha_{\min}$, then the CL objective $\mathcal{L}_{\text{CL}}(\theta)$ upper-bounds the balanced loss $\mathcal{L}_{\text{bal}}(\theta)$ up to an additive θ -independent constant.

Proof Sketch. For the full proof see Appendix B.5. The proof first rewrites the balanced loss as the sum of a Tail term, a Head-loss difference term, and a constant by adding and subtracting $\mathcal{L}_H(\theta_H^*)$. The Tail term $\frac{1}{2}\mathcal{L}_T(\theta)$ is upper-bounded by the task loss $\mathcal{L}_{\text{task}}(\theta)$ and hence by $\mathcal{L}_{\text{CL}}(\theta)$. For the parameter route, local smoothness of \mathcal{L}_H and strong convexity of D_{Ψ} are combined to bound the Head-loss difference in terms of D_{Ψ} , which appears in \mathcal{L}_{CL} when $\beta \geq \beta_{\min}$. For the output route, the calibration inequality bounds the same Head-loss difference in terms of D_{Φ} , controlled by \mathcal{L}_{CL} when $\alpha \geq \alpha_{\min}$. Adding these bounds and the constant yields the dominance relation in Eq. 10.

Under mild, standard local conditions near the Head solution, Theorem 3.10 shows that the unified CL objective (Eq. 6) *upper-bounds* the balanced LTR loss up to a constant as soon as either the parameter penalty weight β exceeds β_{\min} or the output penalty weight α exceeds α_{\min} . We further show in Appendix F.3 that off-the-shelf CL methods typically meet these thresholds by orders of magnitude. Consequently, any optimization procedure that decreases \mathcal{L}_{CL}

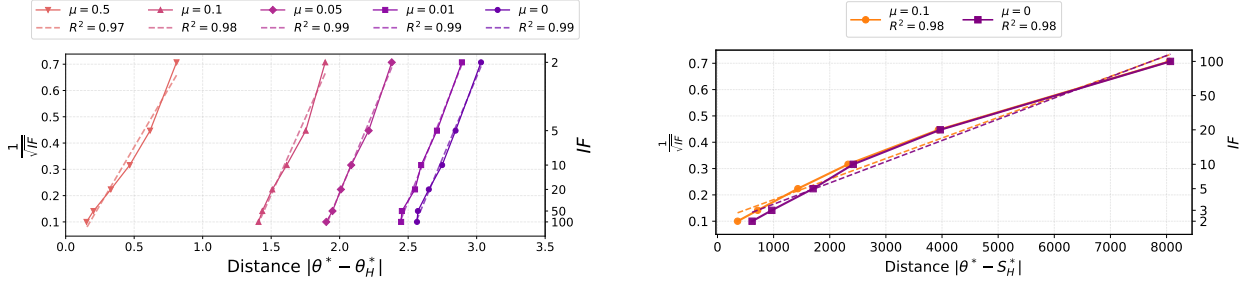


Figure 4: Empirical support for Theorems 3.3 and 3.5. Left: logistic regression on MNIST-LT with varying imbalance factor and different L^2 strengths μ . Right: the same analysis for ResNet-18 on CIFAR-100, with and without weight decay.

(gradient descent or SGD under standard conditions) produces a strictly decreasing sequence $\mathcal{L}_{\text{CL}}(\theta_k) + \frac{1}{2}\mathcal{L}_H(\theta_H^*)$ that *uniformly upper-bounds* $\mathcal{L}_{\text{bal}}(\theta_k)$ along the trajectory. In other words, CL training cannot keep improving \mathcal{L}_{CL} while leaving the balanced LTR loss arbitrarily large; it progressively pushes the model into regions where \mathcal{L}_{bal} is tightly controlled by a decreasing surrogate. Crucially, this surrogate is strictly tighter than necessary: by minimizing the full task loss $\mathcal{L}_{\text{task}}$ (which equals \mathcal{L}_T) rather than the weighted component $\frac{1}{2}\mathcal{L}_T$ inherent to the balanced objective, CLTR effectively prioritizes the Tail. This implicit over-weighting serves as a beneficial corrective mechanism, counteracting the strong Head bias acquired during the initial training stage.

This establishes that off-the-shelf CL methods optimize a surrogate that dominates the balanced LTR objective and therefore *systematically improve* LTR under balanced evaluation. Moreover, in the special convex case analyzed in Appendix B.6, the CL objective coincides with the balanced loss up to an additive constant and thus has *identical minimizers* to the balanced objective. Together, these results provide a theoretical guarantee that using off-the-shelf CL methods for addressing LTR is not ad hoc: CL is revealed as a principled solution to LTR, and in the convex setting it is exactly equivalent to optimizing the balanced LTR loss.

4 Experiments and Results

4.1 Experiment Setup

Datasets. First, we use the **MNIST-LT** [53] toy dataset with different IF values to study the behavior of the upper bound (Eq. 2) and its compliance with our Theorem 3.3. Then we employed **CIFAR100-LT** [15] to numerically verify Theorem 3.5. Next, to evaluate the performance of CLTR in addressing the LTR problem, we employ three widely used LTR datasets: **CIFAR100-LT**, **CIFAR10-LT** [15], and **ImageNet-LT** [11]. These datasets represent long-tailed versions of the original CIFAR100, CIFAR10, and ImageNet datasets, maintaining the same number of classes while the number of samples in each class decreases exponentially according to the IF, where the first class has the maximum number of samples and the last class contains the least number of samples, as illustrated in Appendix D. We also demonstrate the efficacy of CLTR in addressing LT-CIL using the CIFAR100-LT benchmark (Appendix F.1). Finally, to further highlight the benefits of using CLTR, we carry out additional experiments using the naturally skewed **Caltech256** dataset [54] (Appendix F.2).

Implementation Details. Following the experimental setup of [5] and [4], we use ResNet-32 [55] and ResNeXt-50 [56] for CIFAR and ImageNet benchmarks, respectively. The LTR methods selected for comparison are state-of-the-art solutions in the area. We also employ various standard and state-of-the-art CL methods in CLTR, namely LwF [20], EWC [42], Modified EWC [57], GPM [39], FOSTER [38], SGP [47], and TPL [46]. We divided the dataset into 2 partitions for LwF, EWC, Modified EWC, GPM, and SGP and 4 partitions for FOSTER and TPL. All trainings were conducted using an NVIDIA RTX 3090 GPU with 24GB VRAM. More details on the implementation specifics are provided in Appendix C.

Evaluation. For the LTR datasets (MNIST-LT, CIFAR100-LT, CIFAR10-LT, ImageNet-LT), we first train the model on the long-tailed imbalanced training set and then evaluate it on the balanced test set, following the evaluation protocol of [5]. All reported values represent classification accuracy. The results of our proposed approach are highlighted in the Tables.

Table 1: LTR benchmarks for (left) CIFAR100-LT, (middle) CIFAR10-LT, and (right) ImageNet-LT

Model	IF			Model	IF		Model	Top-1 accuracy
	100	50	10		100	50		
Baseline [16]	38.3	43.9	55.7	Baseline [16]	69.8	75.2	Baseline [16]	44.4
Baseline + CB [16]	39.6	45.3	58.0	Baseline + CB [16]	74.7	79.3	Baseline + CB [16]	33.2
Focal loss [28]	38.4	44.3	55.8	Focal loss[28]	70.4	75.3	KD [70]	35.8
Focal+CB [16]	39.6	45.2	58.0	PG Re-sampling [64]	67.1	75.0	Focal [28]	30.5
τ -norm [21]	47.7	52.5	63.8	3LSSL [65]	85.2	88.2	SR Re-sampling [25]	46.8
LDAM-DRW [15]	42.0	46.6	58.7	Focal+CB[16]	74.6	79.3	OLTR [71]	35.6
BBN [18]	42.6	47.0	59.1	LDAM-DRW[15]	77.0	79.3	cRT [21]	49.6
LogitAdjust [58]	42.0	47.0	57.7	BBN [18]	79.8	82.2	τ -norm [21]	49.4
LDAM+SSP [59]	43.4	47.1	58.9	Manifold mixup [16]	73.0	78.1	LFME [72]	37.5
De-confound [17]	44.1	50.3	59.6	CBA-LDAM [16]	80.3	82.2	De-confound [17]	51.8
SSD [60]	46.0	50.5	62.3	ELF (LDAM)+DRW [16]	78.1	82.4	Seasaw Loss [73]	50.4
DiVE [61]	45.4	51.1	62.0	De-confound [17]	80.6	83.6	DiVE [61]	53.1
DRO-LT [62]	47.3	57.6	63.4	Hybrid-SC [66]	81.4	85.4	DisAlign [74]	52.9
WD [5]	46.0	52.7	66.1	MiSLAS [67]	82.1	85.7	WD [5]	48.6
WD & Max [5]	53.4	57.7	68.7	BCL [68]	84.3	87.2	WD+Max [5]	53.9
ABL [26]	46.8	52.1	61.8	FNO [69]	82.6	85.1	ABL [26]	<u>53.2</u>
BS + BSD [31]	50.6	55.4	64.0	BS + BSD [31]	79.7	82.7	EWB-FDR [75]	<u>53.2</u>
PHASE [63]	49.1	52.8	61.2	PHASE [63]	78.9	82.7	SynBalance (n=100) [76]	53.6
CLTR (LwF)	45.1	49.3	58.7	CLTR (LwF)	76.3	78.6	CLTR (LwF)	47.6
CLTR (EWC)	44.4	50.3	58.8	CLTR (EWC)	75.1	80.1	CLTR (EWC)	48.9
CLTR (Modified EWC)	45.9	51.0	60.7	CLTR (Modified EWC)	77.8	81.3	CLTR (Modified EWC)	49.1
CLTR (GPM)	48.3	54.7	64.7	CLTR (GPM)	81.2	84.8	CLTR (GPM)	51.7
CLTR (FOSTER)	48.7	54.4	63.6	CLTR (FOSTER)	81.7	85.9	CLTR (FOSTER)	52.7
CLTR (SGP)	<u>50.7</u>	58.0	<u>67.2</u>	CLTR (SGP)	83.0	85.5	CLTR (SGP)	<u>53.2</u>
CLTR (TPL)	48.4	54.0	62.1	CLTR (TPL)	84.7	87.6	CLTR (TPL)	53.9

4.2 Results

Empirical support for Theorems 3.3 and 3.5. Prior works have shown that complementing theoretical guarantees with focused empirical verification can yield valuable insights into the practical relevance of the theory [77, 78, 79]. Motivated by this, our experiments are structured to test the key behaviors and scaling predicted by our analysis. To evaluate the validity of Theorem 3.3 on the upper bound for the distance between the learner’s weights when trained on \mathcal{D} and \mathcal{D}_H ($\|\theta^* - \theta_H^*\|$), we first train a logistic regression model with cross-entropy loss on MNIST-LT with varying IF to ensure the convexity of the loss function [80]. We use different values for the regularizer coefficient as well (μ). Then, we compute the Euclidean distance between the two sets of weights and plot them against $\frac{1}{\sqrt{\text{IF}}}$, as shown in Fig. 4 top. A regression line is fitted to the data, and the R^2 score is calculated. Consistent with Eq. 2, the difference between the weights is bounded and scales linearly with $\frac{1}{\sqrt{\text{IF}}}$ with high confidence ($R^2 \geq 0.97$). We then extend this experiment to a deeper architecture, ResNet-18 (a feedforward deep network), trained on the CIFAR-100 dataset. We measure the distance $\|\theta^* - \theta_H^*\|$ with and without weight decay and report the results in Fig. 4 bottom. In both settings, the fitted line achieves $R^2 \geq 0.98$, indicating that the bound scales linearly with $\frac{1}{\sqrt{\text{IF}}}$ even in deep networks, where the loss is not convex, as predicted by Theorem 3.5.

Empirical support for Theorems 3.10. We compare the performance of our CLTR framework with existing state-of-the-art LTR solutions on three LTR benchmarks, CIFAR100-LT, CIFAR10-LT, and ImageNet-LT, as presented in Table 1. We also present two additional baselines where we train the backbone model on the imbalanced data, with and without a class-balanced loss term. These results demonstrate that CLTR indeed provides strong performance across all benchmarks, as predicted by our proposed theory.

Following the prior works such as [5], we avoid direct comparisons with solutions with “bells and whistles” such as RIDE [32], ACE [81], SSD [60], and PaCo [82], which employ aggressive data augmentations, ensembles learning, multi-expert and self-supervised pretraining. It is worth mentioning that some previous LTR solutions like BBN [18] learn the Head and Tail separately in a multi-stage manner. They rely on various techniques to prevent performance loss on the Head while learning the Tail. However, unlike these methods, our approach only uses one model through the entire training process, and the results demonstrate that employing standard CL methods yields strong performance in the LTR benchmarks. We further demonstrate the strong performance of CLTR on the more challenging long-tailed class-incremental learning (LT-CIL) benchmarks and on the naturally skewed Caltech256 dataset in Appendices F.1 and F.2, respectively. We also provide additional discussion on the impact of the number of incremental steps (Appendix F.4),

replay memory size (Appendix F.5), runtime (Appendix F.6), weight imbalance (Appendix F.7), and backward/forward transfer as well as catastrophic forgetting (Appendix F.8) to better elucidate the mechanisms underlying CLTR.

5 Conclusion and Future Work

In this work, we considered LTR through the lens of CL. We showed that, under mild assumptions, training on an imbalanced dataset produces parameters that remain in an $\mathcal{O}(1/\sqrt{IF})$ neighborhood of the solution obtained by training on the Head classes alone, both in models with convex loss and standard feedforward models. We further established that a unified CL objective upper-bounds the balanced loss for LTR, providing a principled connection between LTR and CL rather than treating them as separate problems, as has been the case in the literature to date. Building on this perspective, we introduced CLTR as a simple instantiation of this bridge: it first learns the Head, then sequentially incorporates the Tail using off-the-shelf CL techniques to mitigate forgetting. Across CIFAR100-LT, CIFAR10-LT, ImageNet-LT, and Caltech256, as well as LT-CIL benchmarks, our experiments support the theoretical predictions and show that CLTR is competitive with, and in several cases surpasses, strong LTR baselines. This work opens several directions for future research. On the theory side, it would be valuable to relax some of our assumptions, better characterize the constants in our bounds, and extend the analysis beyond classification. On the practical side, combining the CLTR perspective with few-shot, meta, or self-supervised learning could further improve LTR performance. More broadly, we hope that viewing LTR as a CL problem will inspire new algorithms and analyses that jointly advance both fields.

Acknowledgment

We would like to thank Geotab Inc., the City of Kingston, and NSERC for their invaluable and continued support of this work.

References

- [1] Mateusz Buda, Atsuto Maki, and Maciej A Mazurowski. A systematic study of the class imbalance problem in convolutional neural networks. *Neural Networks*, 106:249–259, 2018.
- [2] William J Reed. The pareto, zipf and other power laws. *Economics letters*, 74(1):15–19, 2001.
- [3] Yifan Zhang, Bingyi Kang, Bryan Hooi, Shuicheng Yan, and Jiashi Feng. Deep long-tailed learning: A survey. *IEEE Transactions on Pattern Analysis and Machine Intelligence*, 2023.
- [4] Yu Fu, Liuyu Xiang, Yumna Zahid, Guiguang Ding, Tao Mei, Qiang Shen, and Jungong Han. Long-tailed visual recognition with deep models: A methodological survey and evaluation. *Neurocomputing*, 2022.
- [5] Shaden Alshammari, Yu-Xiong Wang, Deva Ramanan, and Shu Kong. Long-tailed recognition via weight balancing. In *IEEE/CVF Conference on Computer Vision and Pattern Recognition (CVPR)*, pages 6897–6907, 2022.
- [6] Arman Haghanifar, Mahdiyar Molahasani Majdabadi, Younhee Choi, S Deivalakshmi, and Seokbum Ko. Covid-cxnet: Detecting covid-19 in frontal chest x-ray images using deep learning. *Multimedia tools and applications*, 81(21):30615–30645, 2022.
- [7] Wei Cui, Zhanyun Feng, Jiale Chen, Xing Xu, Yueling Tian, Huilin Zhao, and Chenglei Wang. Long-tailed effect study in remote sensing semantic segmentation based on graph kernel principles. *Remote Sensing*, 16(8), 2024.
- [8] Nitesh V Chawla, Kevin W Bowyer, Lawrence O Hall, and W Philip Kegelmeyer. Smote: synthetic minority over-sampling technique. *Journal of Artificial Intelligence Research*, 16:321–357, 2002.
- [9] Andrew Estabrooks, Taeho Jo, and Nathalie Japkowicz. A multiple resampling method for learning from imbalanced data sets. *Computational Intelligence*, 20(1):18–36, 2004.
- [10] Chengjian Feng, Yujie Zhong, and Weilin Huang. Exploring classification equilibrium in long-tailed object detection. In *IEEE/CVF International Conference on Computer Vision (ICCV)*, pages 3417–3426, 2021.
- [11] Ziwei Liu, Zhongqi Miao, Xiaohang Zhan, Jiayun Wang, Boqing Gong, and Stella X Yu. Large-scale long-tailed recognition in an open world. In *IEEE/CVF Conference on Computer Vision and Pattern Recognition (CVPR)*, pages 2537–2546, 2019.
- [12] Yu-Xiong Wang, Deva Ramanan, and Martial Hebert. Learning to model the tail. *Advances in Neural Information Processing Systems (NeurIPS)*, 30, 2017.

- [13] Yaoyao Zhong, Weihong Deng, Mei Wang, Jiani Hu, Jianteng Peng, Xunqiang Tao, and Yaohai Huang. Unequal-training for deep face recognition with long-tailed noisy data. In *IEEE/CVF Conference on Computer Vision and Pattern Recognition (CVPR)*, pages 7812–7821, 2019.
- [14] Muhammad Abdullah Jamal, Matthew Brown, Ming-Hsuan Yang, Liqiang Wang, and Boqing Gong. Rethinking class-balanced methods for long-tailed visual recognition from a domain adaptation perspective. In *IEEE/CVF Conference on Computer Vision and Pattern Recognition (CVPR)*, pages 7610–7619, 2020.
- [15] Kaidi Cao, Colin Wei, Adrien Gaidon, Nikos Arechiga, and Tengyu Ma. Learning imbalanced datasets with label-distribution-aware margin loss. *Advances in Neural Information Processing Systems (NeurIPS)*, 32, 2019.
- [16] Yin Cui, Menglin Jia, Tsung-Yi Lin, Yang Song, and Serge Belongie. Class-balanced loss based on effective number of samples. In *IEEE/CVF Conference on Computer Vision and Pattern Recognition (CVPR)*, pages 9268–9277, 2019.
- [17] Kaihua Tang, Jianqiang Huang, and Hanwang Zhang. Long-tailed classification by keeping the good and removing the bad momentum causal effect. *Advances in Neural Information Processing Systems (NeurIPS)*, 33:1513–1524, 2020.
- [18] Boyan Zhou, Quan Cui, Xiu-Shen Wei, and Zhao-Min Chen. Bbn: Bilateral-branch network with cumulative learning for long-tailed visual recognition. In *IEEE/CVF Conference on Computer Vision and Pattern Recognition (CVPR)*, pages 9719–9728, 2020.
- [19] Yifan Zhang, Bryan Hooi, Lanqing Hong, and Jiashi Feng. Self-supervised aggregation of diverse experts for test-agnostic long-tailed recognition. *Advances in Neural Information Processing Systems (NeurIPS)*, 35:34077–34090, 2022.
- [20] Zhizhong Li and Derek Hoiem. Learning without forgetting. *IEEE Transactions on Pattern Analysis and Machine Intelligence*, 40(12):2935–2947, 2017.
- [21] Bingyi Kang, Saining Xie, Marcus Rohrbach, Zhicheng Yan, Albert Gordo, Jiashi Feng, and Yannis Kalantidis. Decoupling representation and classifier for long-tailed recognition. In *International Conference on Learning Representations (ICLR)*, 2019.
- [22] Hui Han, Wen-Yuan Wang, and Bing-Huan Mao. Borderline-smote: a new over-sampling method in imbalanced data sets learning. In *Advances in Intelligent Computing: International Conference on Intelligent Computing (ICIC)*, pages 878–887, 2005.
- [23] Chris Drummond, Robert C Holte, et al. C4. 5, class imbalance, and cost sensitivity: why under-sampling beats over-sampling. In *Workshop on learning from Imbalanced Datasets II*, volume 11, pages 1–8, 2003.
- [24] Li Shen, Zhouchen Lin, and Qingming Huang. Relay backpropagation for effective learning of deep convolutional neural networks. In *European Conference on Computer Vision (ECCV)*, pages 467–482, 2016.
- [25] Dhruv Mahajan, Ross Girshick, Vignesh Ramanathan, Kaiming He, Manohar Paluri, Yixuan Li, Ashwin Bharambe, and Laurens Van Der Maaten. Exploring the limits of weakly supervised pretraining. In *European Conference on Computer Vision (ECCV)*, pages 181–196, 2018.
- [26] Lianbao Jin, Dayu Lang, and Na Lei. An optimal transport view of class-imbalanced visual recognition. *International Journal of Computer Vision*, 131(11):2845–2863, 2023.
- [27] Chen Huang, Yining Li, Chen Change Loy, and Xiaoou Tang. Deep imbalanced learning for face recognition and attribute prediction. *IEEE Transactions on Pattern Analysis and Machine Intelligence*, 42(11):2781–2794, 2019.
- [28] Tsung-Yi Lin, Priya Goyal, Ross Girshick, Kaiming He, and Piotr Dollár. Focal loss for dense object detection. In *IEEE International Conference on Computer Vision (ICCV)*, pages 2980–2988, 2017.
- [29] Salman Khan, Munawar Hayat, Syed Waqas Zamir, Jianbing Shen, and Ling Shao. Striking the right balance with uncertainty. In *IEEE/CVF Conference on Computer Vision and Pattern Recognition (CVPR)*, pages 103–112, 2019.
- [30] Xi Yin, Xiang Yu, Kihyuk Sohn, Xiaoming Liu, and Manmohan Chandraker. Feature transfer learning for face recognition with under-represented data. In *IEEE/CVF Conference on Computer Vision and Pattern Recognition (CVPR)*, pages 5704–5713, 2019.
- [31] Ning Ren, Xiaosong Li, Yanxia Wu, and Yan Fu. Balanced self-distillation for long-tailed recognition. *Knowledge-Based Systems*, 290:111504, 2024.
- [32] Xudong Wang, Long Lian, Zhongqi Miao, Ziwei Liu, and Stella Yu. Long-tailed recognition by routing diverse distribution-aware experts. In *International Conference on Learning Representations (ICLR)*, 2021.
- [33] Han-Jia Ye, De-Chuan Zhan, and Wei-Lun Chao. Procrustean training for imbalanced deep learning. In *IEEE/CVF International Conference on Computer Vision (ICCV)*, pages 92–102, 2021.

- [34] Emanuele Francazi, Marco Baity-Jesi, and Aurelien Lucchi. A theoretical analysis of the learning dynamics under class imbalance. *International Conference on Machine Learning (ICML)*, 2023.
- [35] Syed Shakib Sarwar, Aayush Ankit, and Kaushik Roy. Incremental learning in deep convolutional neural networks using partial network sharing. *IEEE Access*, 8:4615–4628, 2019.
- [36] Xilai Li, Yingbo Zhou, Tianfu Wu, Richard Socher, and Caiming Xiong. Learn to grow: A continual structure learning framework for overcoming catastrophic forgetting. In *International Conference on Machine Learning (ICML)*, pages 3925–3934, 2019.
- [37] Jaehong Yoon, Saehoon Kim, Eunho Yang, and Sung Ju Hwang. Scalable and order-robust continual learning with additive parameter decomposition. In *Eighth International Conference on Learning Representations (ICLR)*, 2020.
- [38] Fu-Yun Wang, Da-Wei Zhou, Han-Jia Ye, and De-Chuan Zhan. Foster: Feature boosting and compression for class-incremental learning. In *European Conference on Computer Vision (ECCV)*, pages 398–414, 2022.
- [39] Gobinda Saha, Isha Garg, and Kaushik Roy. Gradient projection memory for continual learning. In *International Conference on Learning Representations (ICLR)*, 2020.
- [40] Gobinda Saha, Isha Garg, Aayush Ankit, and Kaushik Roy. Space: Structured compression and sharing of representational space for continual learning. *IEEE Access*, 9:150480–150494, 2021.
- [41] Mehrdad Farajtabar, Navid Azizan, Alex Mott, and Ang Li. Orthogonal gradient descent for continual learning. In *International Conference on Artificial Intelligence and Statistics (AISTATS)*, pages 3762–3773, 2020.
- [42] James Kirkpatrick, Razvan Pascanu, Neil Rabinowitz, Joel Veness, Guillaume Desjardins, Andrei A Rusu, Kieran Milan, John Quan, Tiago Ramalho, Agnieszka Grabska-Barwinska, et al. Overcoming catastrophic forgetting in neural networks. *National Academy of Sciences*, 114(13):3521–3526, 2017.
- [43] Matthew Riemer, Ignacio Cases, Robert Ajemian, Miao Liu, Irina Rish, Yuhai Tu, and Gerald Tesauro. Learning to learn without forgetting by maximizing transfer and minimizing interference. In *International Conference on Learning Representations (ICLR)*, 2018.
- [44] Arslan Chaudhry, Marc’Aurelio Ranzato, Marcus Rohrbach, and Mohamed Elhoseiny. Efficient lifelong learning with a-GEM. In *International Conference on Learning Representations (ICLR)*, 2019.
- [45] Dongsub Shim, Zheda Mai, Jihwan Jeong, Scott Sanner, Hyunwoo Kim, and Jongseong Jang. Online class-incremental continual learning with adversarial shapley value. In *AAAI Conference on Artificial Intelligence*, volume 35, pages 9630–9638, 2021.
- [46] Haowei Lin, Yijia Shao, Weinan Qian, Ningxin Pan, Yiduo Guo, and Bing Liu. Class incremental learning via likelihood ratio based task prediction. In *The Twelfth International Conference on Learning Representations (ICLR)*, 2024.
- [47] Gobinda Saha and Kaushik Roy. Continual learning with scaled gradient projection. *arXiv preprint arXiv:2302.01386*, 2023.
- [48] Yan Hong, Jianfu Zhang, Zhongyi Sun, and Ke Yan. Proaug: Prototype-based augmentation for long-tailed image classification. In *IEEE International Conference on Acoustics, Speech and Signal Processing (ICASSP)*, pages 3035–3039, 2024.
- [49] Damek Davis, Dmitriy Drusvyatskiy, Sham Kakade, and Jason D Lee. Stochastic subgradient method converges on tame functions. *Foundations of computational mathematics*, 20(1):119–154, 2020.
- [50] Tristan Milne. Piecewise strong convexity of neural networks. *Advances in neural information processing systems*, 32, 2019.
- [51] Ameya Prabhu, Philip HS Torr, and Puneet K Dokania. Gdumb: A simple approach that questions our progress in continual learning. In *European Conference on Computer Vision (ECCV)*, pages 524–540, 2020.
- [52] Zhenyi Wang, Yan Li, Li Shen, and Heng Huang. A unified and general framework for continual learning. *arXiv preprint arXiv:2403.13249*, 2024.
- [53] Yann LeCun, Léon Bottou, Yoshua Bengio, and Patrick Haffner. Gradient-based learning applied to document recognition. *IEEE*, 86(11):2278–2324, 1998.
- [54] Gregory Griffin, Alex Holub, and Pietro Perona. Caltech-256 object category dataset. *Technical report*, 2007.
- [55] Kaiming He, Xiangyu Zhang, Shaoqing Ren, and Jian Sun. Deep residual learning for image recognition. In *IEEE Conference on Computer Vision and Pattern Recognition (CVPR)*, pages 770–778, 2016.

- [56] Saining Xie, Ross Girshick, Piotr Dollár, Zhuowen Tu, and Kaiming He. Aggregated residual transformations for deep neural networks. In *IEEE Conference on Computer Vision and Pattern Recognition (CVPR)*, pages 1492–1500, 2017.
- [57] Mahdiyar Molahasani, Ali Etemad, and Michael Greenspan. Continual learning for out-of-distribution pedestrian detection. In *IEEE International Conference on Image Processing (ICIP)*, pages 2685–2689. IEEE, 2023.
- [58] Aditya Krishna Menon, Sadeep Jayasumana, Ankit Singh Rawat, Himanshu Jain, Andreas Veit, and Sanjiv Kumar. Long-tail learning via logit adjustment. In *International Conference on Learning Representations (ICLR)*, 2020.
- [59] Yuzhe Yang and Zhi Xu. Rethinking the value of labels for improving class-imbalanced learning. *Advances in Neural Information Processing Systems (NeurIPS)*, 33:19290–19301, 2020.
- [60] Tianhao Li, Limin Wang, and Gangshan Wu. Self supervision to distillation for long-tailed visual recognition. In *IEEE/CVF International Conference on Computer Vision (ICCV)*, pages 630–639, 2021.
- [61] Yin-Yin He, Jianxin Wu, and Xiu-Shen Wei. Distilling virtual examples for long-tailed recognition. In *IEEE/CVF International Conference on Computer Vision (ICCV)*, pages 235–244, 2021.
- [62] Dvir Samuel and Gal Chechik. Distributional robustness loss for long-tail learning. In *IEEE/CVF International Conference on Computer Vision (ICCV)*, pages 9495–9504, 2021.
- [63] Jiale Li, Jicong Duan, Changbin Shao, and Hualong Yu. Phase: Progressive hierarchical adaptation for sample-efficient rebalancing in long-tail classification. *Symmetry*, 17(12):2040, 2025.
- [64] Yin Cui, Yang Song, Chen Sun, Andrew Howard, and Serge Belongie. Large scale fine-grained categorization and domain-specific transfer learning. In *IEEE Conference on Computer Vision and Pattern Recognition (CVPR)*, pages 4109–4118, 2018.
- [65] Natalia Díaz-Rodríguez, Vincenzo Lomonaco, David Filliat, Davide Maltoni, et al. Don’t forget, there is more than forgetting: new metrics for continual learning. In *Continual Learning Workshop at NeurIPS*, pages 1–7, 2018.
- [66] Peng Wang, Kai Han, Xiu-Shen Wei, Lei Zhang, and Lei Wang. Contrastive learning based hybrid networks for long-tailed image classification. In *IEEE/CVF Conference on Computer Vision and Pattern Recognition (CVPR)*, pages 943–952, 2021.
- [67] Zhisheng Zhong, Jiequan Cui, Shu Liu, and Jiaya Jia. Improving calibration for long-tailed recognition. In *IEEE/CVF Conference on Computer Vision and Pattern Recognition (CVPR)*, pages 16489–16498, 2021.
- [68] Jianggang Zhu, Zheng Wang, Jingjing Chen, Yi-Ping Phoebe Chen, and Yu-Gang Jiang. Balanced contrastive learning for long-tailed visual recognition. In *IEEE/CVF Conference on Computer Vision and Pattern Recognition (CVPR)*, pages 6908–6917, 2022.
- [69] Hoyong Kim and Kangil Kim. Fixed non-negative orthogonal classifier: Inducing zero-mean neural collapse with feature dimension separation. In *The Twelfth International Conference on Learning Representations (ICLR)*, 2024.
- [70] Geoffrey Hinton, Oriol Vinyals, and Jeff Dean. Distilling the knowledge in a neural network. *arXiv preprint arXiv:1503.02531*, 2015.
- [71] Si Liu, Risheek Garrepalli, Thomas Dietterich, Alan Fern, and Dan Hendrycks. Open category detection with pac guarantees. In *International Conference on Machine Learning (ICML)*, pages 3169–3178, 2018.
- [72] Liuyu Xiang, Guiguang Ding, and Jungong Han. Learning from multiple experts: Self-paced knowledge distillation for long-tailed classification. In *European Conference on Computer Vision (ECCV)*, pages 247–263, 2020.
- [73] Jiaqi Wang, Wenwei Zhang, Yuhang Zang, Yuhang Cao, Jiangmiao Pang, Tao Gong, Kai Chen, Ziwei Liu, Chen Change Loy, and Dahua Lin. Seesaw loss for long-tailed instance segmentation. In *IEEE/CVF Conference on Computer Vision and Pattern Recognition (CVPR)*, pages 9695–9704, 2021.
- [74] Songyang Zhang, Zeming Li, Shipeng Yan, Xuming He, and Jian Sun. Distribution alignment: A unified framework for long-tail visual recognition. In *IEEE/CVF Conference on Computer Vision and Pattern Recognition (CVPR)*, pages 2361–2370, 2021.
- [75] Naoya Hasegawa and Issei Sato. Exploring weight balancing on long-tailed recognition problem. In *The Twelfth International Conference on Learning Representations (ICLR)*, 2024.
- [76] Zhongyu Jiang, Jiarui Cai, Chang Liu, Dongsheng An, and Jonathan Wu. Synbalance: Harnessing synthetic data in long-tailed recognition. In *Proceedings of the IEEE/CVF International Conference on Computer Vision*, pages 6276–6285, 2025.

- [77] Farhad Pourpanah, Mahdiyar Molahasani, Milad Soltany, Michael Greenspan, and Ali Etemad. Federated unsupervised domain generalization using global and local alignment of gradients. In *Proceedings of the AAAI Conference on Artificial Intelligence*, volume 39, pages 19948–19958, 2025.
- [78] Jaehoon Lee, Lechao Xiao, Samuel Schoenholz, Yasaman Bahri, Roman Novak, Jascha Sohl-Dickstein, and Jeffrey Pennington. Wide neural networks of any depth evolve as linear models under gradient descent. *Advances in neural information processing systems*, 32, 2019.
- [79] Xinrui Wang, Chuanxing Geng, Wenhai Wan, Shao-Yuan Li, and Songcan Chen. Forgetting, ignorance or myopia: Revisiting key challenges in online continual learning. *Advances in Neural Information Processing Systems*, 37:58341–58375, 2024.
- [80] Marek Rychlik. A proof of convergence of multi-class logistic regression network. *arXiv preprint arXiv:1903.12600*, 2019.
- [81] Jiarui Cai, Yizhou Wang, and Jenq-Neng Hwang. Ace: Ally complementary experts for solving long-tailed recognition in one-shot. In *IEEE/CVF International Conference on Computer Vision (ICCV)*, pages 112–121, 2021.
- [82] Jiequan Cui, Zhisheng Zhong, Shu Liu, Bei Yu, and Jiaya Jia. Parametric contrastive learning. In *IEEE/CVF International Conference on Computer Vision (ICCV)*, pages 715–724, 2021.
- [83] Chris Dongjoo Kim, Jinseo Jeong, and Gunhee Kim. Imbalanced continual learning with partitioning reservoir sampling. In *European Conference on Computer Vision (ECCV)*, pages 411–428, 2020.
- [84] Xialei Liu, Yu-Song Hu, Xu-Sheng Cao, Andrew D Bagdanov, Ke Li, and Ming-Ming Cheng. Long-tailed class incremental learning. In *European Conference on Computer Vision (ECCV)*, pages 495–512, 2022.
- [85] Ziwei Liu, Zhongqi Miao, Xiaohang Zhan, Jiayun Wang, Boqing Gong, and X Yu Stella. Open long-tailed recognition in a dynamic world. *IEEE Transactions on Pattern Analysis and Machine Intelligence*, 2022.
- [86] Saihui Hou, Xinyu Pan, Chen Change Loy, Zilei Wang, and Dahua Lin. Learning a unified classifier incrementally via rebalancing. In *IEEE/CVF Conference on Computer Vision and Pattern Recognition (CVPR)*, pages 831–839, 2019.
- [87] Arthur Douillard, Matthieu Cord, Charles Ollion, Thomas Robert, and Eduardo Valle. Podnet: Pooled outputs distillation for small-tasks incremental learning. In *European Conference on Computer Vision (ECCV)*, pages 86–102, 2020.
- [88] Francisco M Castro, Manuel J Marín-Jiménez, Nicolás Guil, Cordelia Schmid, and Karteek Alahari. End-to-end incremental learning. In *European Conference on Computer Vision (ECCV)*, pages 233–248, 2018.
- [89] Xingjian Li, Haoyi Xiong, Hanchao Wang, Yuxuan Rao, Liping Liu, and Jun Huan. Delta: Deep learning transfer using feature map with attention for convolutional networks. In *International Conference on Learning Representations (ICLR)*, 2018.
- [90] Bingyan Liu, Yifeng Cai, Yao Guo, and Xiangqun Chen. Transtailor: Pruning the pre-trained model for improved transfer learning. In *AAAI Conference on Artificial Intelligence*, volume 35, pages 8627–8634, 2021.
- [91] Sen Lin, Li Yang, Deliang Fan, and Junshan Zhang. Beyond not-forgetting: Continual learning with backward knowledge transfer. *Advances in Neural Information Processing Systems (NeurIPS)*, 35:16165–16177, 2022.

Appendix

A Notation

Here, we summarize the key notations used throughout the paper:

- $|\cdot|$: Denotes the cardinality of a set, i.e., the number of elements in the set.
- $\|\cdot\|$: Denotes the L_2 norm.
- $\mathcal{O}(\cdot)$: Denotes the asymptotic upper bound of a function.
- $\mathcal{D} = \{(x_i, y_i)_{i=1}^n\}$: Dataset, where $n = |\mathcal{D}|$.
- $\mathcal{D}_c = \{(x_i, y_i) \in \mathcal{D} \mid y_i = c\}$: Subgroup of \mathcal{D} elements belonging to class c .
- c_k : Number of Head classes.
- $\mathcal{D}_H = \{(x_i, y_i) \in \mathcal{D} : y_i \leq c_k\}$: Head set.
- $\mathcal{D}_T = \{(x_i, y_i) \in \mathcal{D} : y_i > c_k\}$: Tail set.
- \mathcal{D}^i : The i^{th} partition of \mathcal{D} .
- κ : Number of samples in each class of the test set.
- IF : Imbalance factor.
- $\text{IF}_{\mathcal{D}^1, \mathcal{D}^2} = \frac{|\mathcal{D}^1|}{|\mathcal{D}^2|}$: Imbalance factor between two partitions of the dataset.
- $c^{\max} = \arg \max_c |\mathcal{D}_c|$: The class with the most number of samples.
- $c^{\min} = \arg \min_c |\mathcal{D}_c|$: The class with the least number of samples.
- $\ell((x_i, y_i), \theta)$: Loss over one single data point.
- $\ell_{(x_i, y_i)}(\theta) = \ell((x_i, y_i), \theta)$: Alternative notation for loss over a single data point.
- $\mathcal{L}(\mathcal{D}_c, \theta) = \frac{1}{|\mathcal{D}_c|} \sum_{(x_i, y_i) \in \mathcal{D}_c} \ell((x_i, y_i), \theta)$: Average loss function over $\mathcal{D}_c \subset \mathcal{D}$.
- $\mathcal{L}_{\mathcal{D}_c} = \mathcal{L}_{\mathcal{D}_c}(\theta) = \mathcal{L}(\mathcal{D}_c, \theta)$: Alternative notations for the loss function over \mathcal{D}_c .
- $\mathcal{L}(\theta) := \mathcal{L}(\mathcal{D}, \theta)$: (Regularized) average loss over the full dataset \mathcal{D} .
- $\mathcal{L}_H(\theta) := \mathcal{L}(\mathcal{D}_H, \theta)$: Average loss over the Head set.
- $\mathcal{L}_T(\theta) := \mathcal{L}(\mathcal{D}_T, \theta)$: Average loss over the Tail set.
- $\mathcal{L}_{\text{bal}}(\theta) := \frac{1}{2}\mathcal{L}_T(\theta) + \frac{1}{2}\mathcal{L}_H(\theta)$: Balanced loss combining Head and Tail.
- $\mathcal{L}_{\text{task}}(\theta)$: Task loss used in the CL objective (equal to \mathcal{L}_T in CLTR stage-2).
- $\mathcal{L}_{\text{CL}}(\theta)$: Unified continual-learning objective used in CLTR.
- $D_\Phi(\cdot, \cdot)$: Bregman divergence in output space generated by a convex C^1 function Φ .
- $D_\Psi(\cdot, \cdot)$: Bregman divergence in parameter space generated by a convex C^1 function Ψ .
- $D_{\mathcal{L}_H}(\theta, \theta_H^*)$: Bregman divergence generated by the Head loss \mathcal{L}_H .
- Φ, Ψ : Convex C^1 generator functions for the Bregman divergences D_Φ and D_Ψ .
- $\frac{\mu}{2}$: Coefficient of L^2 -norm regularization.
- θ : Parameter vector of the model.
- θ^i : Parameter vector of the model after the i^{th} iteration of training.
- θ^* (also written θ^*) : Parameter vector of the model after training on \mathcal{D} .
- θ_H^* (also written θ_H^*) : Parameter vector of the model after training on \mathcal{D}_H (Head-only optimum).
- θ_T^* : Parameter vector of the model after training on \mathcal{D}_T .
- θ_{HT}^* : Parameter vector of the model optimal for both \mathcal{D}_H and \mathcal{D}_T .
- $\theta_{H,k}^*$: k^{th} local minimizer of the Head loss in the non-convex setting.
- $h_\theta(\cdot)$: Model (neural network) mapping an input to its prediction/logits.
- ψ_H : Region in weight space where the network performs well on the Head set.

- ψ_T : Region in weight space where the network performs well on the Tail set.
- ψ_{HT} : Intersection of ψ_H and ψ_T .
- \mathcal{Y}_t : Set of the labels corresponding to step t in the CL setting.
- \mathcal{M} : Replay memory.
- F : Fisher information matrix.
- H_H : Positive-definite matrix (e.g., empirical Fisher/Hessian) used in the quadratic/EWC-style regularizer $\Psi(\theta) = \frac{1}{2}(\theta - \theta_H^*)^\top H_H(\theta - \theta_H^*)$.
- S_H : Set of minimizers of the Head loss \mathcal{L}_H (or of \mathcal{L} restricted to \mathcal{D}_H).
- $\text{dist}(\theta, S_H)$: Euclidean distance from parameter vector θ to the set S_H .
- C : Positive constant in the Hölder-1/2 error bound linking $\text{dist}(\theta^*, S_H)$ to the Head-loss gap.
- M : Positive constant in the bound $\max_\theta |\mathcal{L}(\mathcal{D}) - \mathcal{L}(\mathcal{D}_H)| = \frac{M}{1+\text{IF}}$.
- $\mathcal{N} \subset \mathbb{R}^d$: Neighborhood of θ_H^* where Assumption 3.9 holds.
- L_H^{sm} : Local smoothness constant of \mathcal{L}_H at θ_H^* .
- m_Ψ : Strong-convexity constant of $D_\Psi(\cdot, \theta_H^*)$.
- c_Φ : Calibration constant relating \mathcal{L}_H to D_Φ .
- α, β : Non-negative weights of the output and parameter regularization terms in \mathcal{L}_{CL} .
- $\beta_{\min} := \frac{L_H^{\text{sm}}}{2m_\Psi}$: Threshold on β ensuring the parameter-route dominance guarantee.
- $\alpha_{\min} := \frac{c_\Phi}{2}$: Threshold on α ensuring the output-route dominance guarantee.
- k_T : Number of classes in the Tail.
- k_H : Number of classes in the Head.

B Proofs

Here we provide proofs for all the theorems. For convenience, we restate each theorem at the start of its corresponding section before presenting the proof.

B.1 Proof of Theorem 3.3

Theorem (Theorem 3.3 (restated)). Given Assumption 3.2, if a model is trained in an LTR setting (Definition 3.1), then the weights of the model after training (θ^*) will lie within the bounded neighborhood of the model’s weight if solely trained on Head (θ_H^*), with the scale of:

$$\|\theta^* - \theta_H^*\| = \mathcal{O}\left(\frac{1}{\sqrt{\text{IF}}}\right). \quad (11)$$

Proof of Theorem 3.3. Following Assumption 3.2, the model is trained on the entire dataset \mathcal{D} by minimizing the loss function \mathcal{L}_T , which can be formulated as:

$$\mathcal{L}_{\text{total}}(\mathcal{D}) = \mathcal{L}(\mathcal{D}) + \frac{\mu}{2}\|\theta\|^2, \quad (12)$$

The loss $\mathcal{L}(\mathcal{D})$ can be decomposed as:

$$\mathcal{L}(\mathcal{D}) = \frac{1}{|\mathcal{D}|} \left(\sum_{(\mathbf{x}_i, y_i) \in \mathcal{D}_H} \ell((\mathbf{x}_i, y_i)) + \sum_{(\mathbf{x}_i, y_i) \in \mathcal{D}_T} \ell((\mathbf{x}_i, y_i)) \right), \quad (13)$$

Using $\mathcal{L}(\mathcal{D}_H) = \frac{1}{|\mathcal{D}_H|} \sum_{(\mathbf{x}_i, y_i) \in \mathcal{D}_H} \ell((\mathbf{x}_i, y_i))$ and $\mathcal{L}(\mathcal{D}_T) = \frac{1}{|\mathcal{D}_T|} \sum_{(\mathbf{x}_i, y_i) \in \mathcal{D}_T} \ell((\mathbf{x}_i, y_i))$, we can rewrite $\mathcal{L}(\mathcal{D})$ as:

$$\mathcal{L}(\mathcal{D}) = \frac{|\mathcal{D}_H|}{|\mathcal{D}|} \mathcal{L}(\mathcal{D}_H) + \frac{|\mathcal{D}_T|}{|\mathcal{D}|} \mathcal{L}(\mathcal{D}_T). \quad (14)$$

Let $\gamma = \frac{|\mathcal{D}_H|}{|\mathcal{D}|}$. Since $|\mathcal{D}| = |\mathcal{D}_H| + |\mathcal{D}_T|$, we can derive that $1 - \gamma = \frac{|\mathcal{D}_T|}{|\mathcal{D}|}$. Plugging γ into Eq. 14 yields:

$$\mathcal{L}(\mathcal{D}) = \gamma \mathcal{L}(\mathcal{D}_H) + (1 - \gamma) \mathcal{L}(\mathcal{D}_T). \quad (15)$$

We now express γ in terms of the imbalance factor IF in Definition 3.1 under the LTR setting. Let k_H and k_T denote the number of Head and Tail classes, respectively ($k_H + k_T = k$). Under Assumption 3.2 (LTR setting with approximately constant per-class sizes within Head and within Tail), let n_H be the number of samples per Head class and n_T be the number of samples per Tail class. Then $|\mathcal{D}_H| = k_H n_H$ and $|\mathcal{D}_T| = k_T n_T$. Moreover, by Definition 3.1, $\text{IF} = \frac{n_H}{n_T}$, hence

$$\gamma = \frac{|\mathcal{D}_H|}{|\mathcal{D}_H| + |\mathcal{D}_T|} = \frac{k_H n_H}{k_H n_H + k_T n_T} = \frac{k_H \text{IF}}{k_H \text{IF} + k_T}, \quad (16)$$

and therefore

$$1 - \gamma = \frac{k_T}{k_H \text{IF} + k_T}. \quad (17)$$

Since in LTR we have $\text{IF} \gg 1$ (Definition 3.1), $\gamma \rightarrow 1$ and $1 - \gamma = \mathcal{O}(1/\text{IF})$. Consequently, $\mathcal{L}(\mathcal{D})$ approaches $\mathcal{L}(\mathcal{D}_H)$ for all θ values.

Let δ represent the maximum difference between the losses:

$$\delta = \max_{\theta} |\mathcal{L}(\mathcal{D}) - \mathcal{L}(\mathcal{D}_H)|. \quad (18)$$

From Eq. 15, it follows that as $\text{IF} \rightarrow \infty$, $\delta \rightarrow 0$. To find the asymptotic relationship of δ with IF, we derive:

$$|\mathcal{L}(\mathcal{D}) - \mathcal{L}(\mathcal{D}_H)| = |(1 - \gamma)(\mathcal{L}(\mathcal{D}_T) - \mathcal{L}(\mathcal{D}_H))|, \quad (19)$$

Replacing $1 - \gamma$ with $\frac{k_T}{k_H \text{IF} + k_T}$ from Eq. 17 and simplifying:

$$|\mathcal{L}(\mathcal{D}) - \mathcal{L}(\mathcal{D}_H)| = \frac{k_T}{k_H \text{IF} + k_T} |\mathcal{L}(\mathcal{D}_T) - \mathcal{L}(\mathcal{D}_H)|. \quad (20)$$

By applying maximization over θ , we derive:

$$\max_{\theta} |\mathcal{L}(\mathcal{D}) - \mathcal{L}(\mathcal{D}_H)| = \frac{k_T}{k_H \text{IF} + k_T} \max_{\theta} |\mathcal{L}(\mathcal{D}_T) - \mathcal{L}(\mathcal{D}_H)|. \quad (21)$$

Since IF is independent of θ :

$$\max_{\theta} |\mathcal{L}(\mathcal{D}) - \mathcal{L}(\mathcal{D}_H)| = M \frac{k_T}{k_H \text{IF} + k_T}, \quad (22)$$

where $M = \max_{\theta} (|\mathcal{L}(\mathcal{D}_T) - \mathcal{L}(\mathcal{D}_H)|)$. We assume $M < \infty$ (e.g., ℓ is bounded/clipped or the optimization domain is restricted). Since $\mathcal{L}(\mathcal{D}_T)$ and $\mathcal{L}(\mathcal{D}_H)$ are average loss over Head and Tail, respectively, they are independent of IF. Moreover, number of classes in the Head (k_H) and number of classes in the Tail (k_T) are also independent of IF. Consequently, replacing δ from Eq. 18 in Eq. 22 yields:

$$\delta = \mathcal{O}\left(\frac{1}{\text{IF}}\right). \quad (23)$$

Adding and subtracting the regularizer $\frac{\mu}{2} \|\theta\|^2$ in Eq. 18 yields:

$$\delta = \max_{\theta} |\mathcal{L}_T(\mathcal{D}) - \mathcal{L}_T(\mathcal{D}_H)|. \quad (24)$$

We now use the following lemma to relate the difference in losses to the difference in the parameter vectors:

Lemma B.1. *If $|f(x) - g(x)| \leq \delta$ for all $x \in \mathbb{R}^d$, then:*

$$\|x_f - x_g\|^2 \leq \frac{4\delta}{\lambda_f + \lambda_g}, \quad (25)$$

where $x_g = \arg \min g(x)$, $x_f = \arg \min f(x)$, and λ_f, λ_g are the minimum eigenvalues of the Hessians of $f(x)$ and $g(x)$, respectively. (For full proof see B.2.)

Applying Lemma B.1 to Eq. 24, we get:

$$\|\theta^* - \theta_H^*\|^2 \leq \frac{4\delta}{\lambda + \lambda_H}, \quad (26)$$

where λ and λ_H are the minimum eigenvalues of the Hessians of $\mathcal{L}_T(\mathcal{D})$ and $\mathcal{L}_T(\mathcal{D}_H)$, respectively.

To find λ and λ_H , note that:

$$\nabla^2 \mathcal{L}_T(\mathcal{D}) = \nabla^2 \mathcal{L}(\mathcal{D}) + \mu \mathbf{I}, \quad \nabla^2 \mathcal{L}_T(\mathcal{D}_H) = \nabla^2 \mathcal{L}(\mathcal{D}_H) + \mu \mathbf{I}, \quad (27)$$

Since $\nabla^2 \mathcal{L}(\mathcal{D}) \succeq 0$ and $\nabla^2 \mathcal{L}(\mathcal{D}_H) \succeq 0$ due to the fact that $\mathcal{L}(\cdot)$ is convex, we have $\lambda, \lambda_H \geq \mu$.

Substituting this back into Eq. 26 yields:

$$\|\theta^* - \theta_H^*\|^2 \leq \frac{2\delta}{\mu}. \quad (28)$$

From Eq. 23, $\delta = \mathcal{O}(\frac{1}{\text{IF}})$, so:

$$\|\theta^* - \theta_H^*\|^2 = \mathcal{O}\left(\frac{1}{\text{IF}}\right). \quad (29)$$

According to Definition 3.1, $\text{IF} \gg 1$, consequently:

$$\|\theta^* - \theta_H^*\| = \mathcal{O}\left(\frac{1}{\sqrt{\text{IF}}}\right). \quad (30)$$

Eq. 30 and Eq. 28 complete the proof. \square

B.2 Proof of Lemma B.1

Proof. Using the second-order Taylor series expansion for multivariate functions, we can approximate $f(x_g)$ and $g(x_f)$ as follows:

$$f(x_g) \simeq f(x_f) + \nabla f(x_f)(x_g - x_f) + \frac{1}{2}(x_g - x_f)^\top H_f(x_f)(x_g - x_f), \quad (31)$$

$$g(x_f) \simeq g(x_g) + \nabla g(x_g)(x_f - x_g) + \frac{1}{2}(x_f - x_g)^\top H_g(x_g)(x_f - x_g), \quad (32)$$

where $H_f(x_f)$ and $H_g(x_g)$ are the Hessian matrices of f and g evaluated at x_f and x_g , respectively.

Since $\nabla f(x_f) = \nabla g(x_g) = 0$, by adding Eq. 31 and Eq. 32 together, we obtain:

$$f(x_g) - g(x_g) + g(x_f) - f(x_f) \simeq \frac{1}{2}(x_g - x_f)^\top H_f(x_f)(x_g - x_f) + \frac{1}{2}(x_f - x_g)^\top H_g(x_g)(x_f - x_g), \quad (33)$$

Using $|f(x) - g(x)| \leq \delta$, we can maximize $(g(x_f) - f(x_f))$ and $(f(x_g) - g(x_g))$:

$$2\delta \geq \frac{1}{2}(x_g - x_f)^\top H_f(x_f)(x_g - x_f) + \frac{1}{2}(x_f - x_g)^\top H_g(x_g)(x_f - x_g), \quad (34)$$

Let λ_f and λ_g be the minimum eigenvalues of $H_f(x_f)$ and $H_g(x_g)$, respectively. By properties of the minimum eigenvalues, we can say:

$$(x_g - x_f)^\top H_f(x_f)(x_g - x_f) \geq \lambda_f \|x_g - x_f\|^2, \quad (35)$$

$$(x_f - x_g)^\top H_g(x_g)(x_f - x_g) \geq \lambda_g \|x_f - x_g\|^2. \quad (36)$$

Using Eqs. 35 and 36, we can rewrite Eq. 34:

$$2\delta \geq \frac{1}{2}\lambda_f \|x_g - x_f\|^2 + \frac{1}{2}\lambda_g \|x_f - x_g\|^2. \quad (37)$$

Therefore:

$$\|x_f - x_g\|^2 \leq \frac{4\delta}{\lambda_f + \lambda_g}, \quad (38)$$

which completes the proof. \square

B.3 Proof of Theorem 3.5

Theorem (Theorem 3.5 (restated)). Given Assumption 3.4, there exists a bound for the distance between the weights of the model after training (θ^*) and one of the minima of the loss landscape when training on the head solely, scaling inversely with the square root of the imbalance factor:

$$\text{dist}(\theta^*, S_H) = \mathcal{O}\left(\frac{1}{\sqrt{\text{IF}}}\right). \quad (39)$$

Proof. Following assumption 3.4, \mathcal{L} has the KL property with an exponent of 1/2. Since the loss is regularized with L^2 regularization, the total loss function is proved to be piecewise strongly convex [50]. Hence, a Hölder–1/2 error bound holds for the loss function \mathcal{L}_H :

$$\text{dist}(\theta^*, S_H) \leq C\sqrt{\mathcal{L}_H(\theta^*) - \mathcal{L}_H(\theta_H^*)} \quad \text{for all } \theta_H^* \in S_H, \quad (40)$$

where C is a constant. Let θ_H^* be any element in S_H . Since θ^* is the minimizer of \mathcal{L} , by optimality we have:

$$\mathcal{L}(\theta^*) \leq \mathcal{L}(\theta_H^*) \quad (41)$$

We seek to bound the term $\mathcal{L}_H(\theta^*) - \mathcal{L}_H(\theta_H^*)$. We can add and subtract terms to decompose it:

$$\mathcal{L}_H(\theta^*) - \mathcal{L}_H(\theta_H^*) = (\mathcal{L}_H(\theta^*) - \mathcal{L}(\theta^*)) + (\mathcal{L}(\theta^*) - \mathcal{L}(\theta_H^*)) + (\mathcal{L}(\theta_H^*) - \mathcal{L}_H(\theta_H^*)) \quad (42)$$

From the optimality of θ^* , we know the middle term is non-positive: $(\mathcal{L}(\theta^*) - \mathcal{L}(\theta_H^*)) \leq 0$. We can thus bound the expression by dropping this term:

$$\mathcal{L}_H(\theta^*) - \mathcal{L}_H(\theta_H^*) \leq (\mathcal{L}_H(\theta^*) - \mathcal{L}(\theta^*)) + (\mathcal{L}(\theta_H^*) - \mathcal{L}_H(\theta_H^*)) \quad (43)$$

We now apply the bound from Eq. 22 ($\max_{\theta} |\mathcal{L}(\mathcal{D}) - \mathcal{L}(\mathcal{D}_H)| = M \frac{k_T}{k_H \text{IF} + k_T}$) to both terms on the right-hand side:

$$(\mathcal{L}_H(\theta^*) - \mathcal{L}(\theta^*)) \leq |\mathcal{L}_H(\theta^*) - \mathcal{L}(\theta^*)| \leq M \frac{k_T}{k_H \text{IF} + k_T} \quad (44)$$

$$(\mathcal{L}(\theta_H^*) - \mathcal{L}_H(\theta_H^*)) \leq |\mathcal{L}(\theta_H^*) - \mathcal{L}_H(\theta_H^*)| \leq M \frac{k_T}{k_H \text{IF} + k_T} \quad (45)$$

Substituting these bounds back gives:

$$\mathcal{L}_H(\theta^*) - \mathcal{L}_H(\theta_H^*) \leq M \frac{k_T}{k_H \text{IF} + k_T} + M \frac{k_T}{k_H \text{IF} + k_T} = 2M \frac{k_T}{k_H \text{IF} + k_T} \quad (46)$$

Replacing the result from Eq. 46 into the error bound Eq. 40 yields:

$$\text{dist}(\theta^*, S_H) \leq C\sqrt{\mathcal{L}_H(\theta^*) - \mathcal{L}_H(\theta_H^*)} \leq C\sqrt{2M \frac{k_T}{k_H \text{IF} + k_T}} \quad (47)$$

Consequently:

$$\text{dist}(\theta^*, S_H) = \mathcal{O}\left(\frac{1}{\sqrt{\text{IF}}}\right), \quad (48)$$

which completes the proof. \square

B.4 Proof of Theorem 3.7

Theorem (Theorem 3.7 (restated)). Following Assumption 3.6, when dataset \mathcal{D} is divided into n partitions sorted based on their cardinality, i.e. $|\mathcal{D}^i| > |\mathcal{D}^j|$ for all $i < j$, then, the weights θ^* obtained from training the model on \mathcal{D} will always be in a bounded neighborhood of the weights $\theta_{\mathcal{D}^1}^*$ obtained from training on the largest subset of \mathcal{D} with the scale of:

$$\begin{aligned} \|\theta_{\mathcal{D}^1}^* - \theta^*\| &= \sum_{i=2}^n \mathcal{O}\left(\sqrt{\frac{|\mathcal{D}^i|}{\sum_{j=1}^{i-1} |\mathcal{D}^j|}}\right) \\ &\approx \mathcal{O}\left(\frac{1}{\sqrt{\text{IF}_{\mathcal{D}^1, \mathcal{D}^2}}}\right), \end{aligned} \quad (49)$$

where $\text{IF}_{\mathcal{D}^1, \mathcal{D}^2} = \frac{|\mathcal{D}^1|}{|\mathcal{D}^2|}$.

Proof of Theorem 3.7. We aim to show that the weights θ^* , obtained from training on the full dataset \mathcal{D} , are in a bounded neighborhood of the weights $\theta_{\mathcal{D}^1}^*$, obtained from training on the largest partition \mathcal{D}^1 . Since each partition is no longer long-tailed, we estimate the cardinality of each partition as the average of the cardinality of the classes within each partition, hence, we assume all classes within each partition have the same of samples $|\mathcal{D}_c| = |\mathcal{D}^i|$ for $\mathcal{D}_c \in \mathcal{D}^i$.

We divide \mathcal{D} into n partitions $\{\mathcal{D}^1, \mathcal{D}^2, \dots, \mathcal{D}^n\}$, sorted by cardinality such that $|\mathcal{D}^1| > |\mathcal{D}^2| > \dots > |\mathcal{D}^n|$. For each consecutive pair, we apply Theorem 3.3:

$$\|\theta_{\mathcal{D}^1}^* - \theta_{\mathcal{D}^1 \cup \mathcal{D}^2}^*\| = \mathcal{O}\left(\sqrt{\frac{|\mathcal{D}^2|}{|\mathcal{D}^1|}}\right), \quad (50)$$

$$\|\theta_{\mathcal{D}^1 \cup \mathcal{D}^2}^* - \theta_{\mathcal{D}^1 \cup \mathcal{D}^2 \cup \mathcal{D}^3}^*\| = \mathcal{O}\left(\sqrt{\frac{|\mathcal{D}^3|}{|\mathcal{D}^1| + |\mathcal{D}^2|}}\right), \quad (51)$$

⋮

$$\|\theta_{\mathcal{D}^1 \cup \dots \cup \mathcal{D}^{i-1}}^* - \theta_{\mathcal{D}^1 \cup \dots \cup \mathcal{D}^i}^*\| = \mathcal{O}\left(\sqrt{\frac{|\mathcal{D}^i|}{\sum_{j=1}^{i-1} |\mathcal{D}^j|}}\right). \quad (52)$$

Using the triangle inequality for norms, the total distance between $\theta_{\mathcal{D}^1}^*$ and $\theta_{\mathcal{D}}^*$ is bounded by the sum of the distances across all steps:

$$\|\theta_{\mathcal{D}^1}^* - \theta_{\mathcal{D}}^*\| \leq \sum_{i=2}^n \|\theta_{\mathcal{D}^1 \cup \dots \cup \mathcal{D}^{i-1}}^* - \theta_{\mathcal{D}^1 \cup \dots \cup \mathcal{D}^i}^*\|. \quad (53)$$

Substituting Eq. 52 into Eq. 53, we get:

$$\|\theta_{\mathcal{D}^1}^* - \theta_{\mathcal{D}}^*\| = \sum_{i=2}^n \mathcal{O}\left(\sqrt{\frac{|\mathcal{D}^i|}{\sum_{j=1}^{i-1} |\mathcal{D}^j|}}\right). \quad (54)$$

For the first step (from \mathcal{D}^1 to $\mathcal{D}^1 \cup \mathcal{D}^2$), the imbalance factor is:

$$\text{IF}_{\mathcal{D}^1, \mathcal{D}^2} = \frac{|\mathcal{D}^1|}{|\mathcal{D}^2|}. \quad (55)$$

From Eq. 50, the distance is:

$$\|\theta_{\mathcal{D}^1}^* - \theta_{\mathcal{D}^1 \cup \mathcal{D}^2}^*\| = \mathcal{O}\left(\sqrt{\frac{1}{\text{IF}_{\mathcal{D}^1, \mathcal{D}^2}}}\right). \quad (56)$$

For subsequent steps, the effective imbalance factor is:

$$\text{IF}_{\text{effective}}^{(i)} = \frac{\sum_{j=1}^{i-1} |\mathcal{D}^j|}{|\mathcal{D}^i|}. \quad (57)$$

Thus, each term in the sum Eq. 54 is of the form:

$$\|\theta_{\mathcal{D}^1 \cup \dots \cup \mathcal{D}^{i-1}}^* - \theta_{\mathcal{D}^1 \cup \dots \cup \mathcal{D}^i}^*\| = \mathcal{O}\left(\sqrt{\frac{1}{\text{IF}_{\text{effective}}^{(i)}}}\right). \quad (58)$$

Combining all contributions, the total distance becomes:

$$\|\theta_{\mathcal{D}^1}^* - \theta_{\mathcal{D}}^*\| = \sum_{i=2}^n \mathcal{O}\left(\sqrt{\frac{1}{\text{IF}_{\text{effective}}^{(i)}}}\right). \quad (59)$$

For simplicity, the dominant term in the sum arises from the first imbalance factor $\text{IF}_{\mathcal{D}^1, \mathcal{D}^2}$ because $\text{IF}_{\mathcal{D}^1, \mathcal{D}^2} \gg \text{IF}_{\text{effective}}^{(i)}$ for $i > 2$. Hence, we can approximate:

$$\|\theta_{\mathcal{D}^1}^* - \theta_{\mathcal{D}}^*\| \approx \mathcal{O}\left(\frac{1}{\sqrt{\text{IF}_{\mathcal{D}^1, \mathcal{D}^2}}}\right). \quad (60)$$

The weights θ^* obtained from training on the full dataset \mathcal{D} reside in a bounded neighborhood of the weights $\theta_{\mathcal{D}^1}^*$, with the total distance given by:

$$\|\theta_{\mathcal{D}^1}^* - \theta^*\| = \sum_{i=2}^n \mathcal{O} \left(\sqrt{\frac{|\mathcal{D}^i|}{\sum_{j=1}^{i-1} |\mathcal{D}^j|}} \right) \approx \mathcal{O} \left(\frac{1}{\sqrt{\mathbf{IF}_{\mathcal{D}^1, \mathcal{D}^2}}} \right), \quad (61)$$

which completes the proof. \square

B.5 Proof of Theorem 3.10

Theorem (Theorem 3.10 (restated)). Suppose Assumption 3.9 holds on \mathcal{N} . Define the thresholds

$$\beta_{\min} := \frac{L_H^{\text{sm}}}{2m_\Psi}, \quad \alpha_{\min} := \frac{c_\Phi}{2},$$

where L_H^{sm} is local smoothness constant of \mathcal{L}_H at θ_H^* , m_Ψ is strong-convexity constant of $D_\Psi(\cdot, \theta_H^*)$, and c_Φ is calibration constant relating \mathcal{L}_H to D_Φ . If either $\beta \geq \beta_{\min}$ (Parameter route) or $\alpha \geq \alpha_{\min}$ (Output route), then for any $\theta \in \mathcal{N}$,

$$\mathcal{L}_{\text{bal}}(\theta) \leq \mathcal{L}_{\text{CL}}(\theta) + \frac{1}{2} \mathcal{L}_H(\theta_H^*). \quad (62)$$

In words: if either $\beta \geq \beta_{\min}$ or $\alpha \geq \alpha_{\min}$, then the CL objective $\mathcal{L}_{\text{CL}}(\theta)$ upper-bounds the balanced loss $\mathcal{L}_{\text{bal}}(\theta)$ up to an additive θ -independent constant.

Proof. We first prove the dominance inequality Eq. 10. Recall

$$\mathcal{L}_{\text{bal}}(\theta) := \frac{1}{2} \mathcal{L}_T(\theta) + \frac{1}{2} \mathcal{L}_H(\theta),$$

and add/subtract $\mathcal{L}_H(\theta_H^*)$:

$$\mathcal{L}_{\text{bal}}(\theta) = \frac{1}{2} \mathcal{L}_T(\theta) + \frac{1}{2} (\mathcal{L}_H(\theta) - \mathcal{L}_H(\theta_H^*)) + \frac{1}{2} \mathcal{L}_H(\theta_H^*). \quad (63)$$

Since $\mathcal{L}_{\text{task}} \equiv \mathcal{L}_T$ and the loss is non-negative, we have

$$\frac{1}{2} \mathcal{L}_T(\theta) \leq \mathcal{L}_{\text{task}}(\theta), \quad (64)$$

and combining Eq. 63 and Eq. 64 gives

$$\mathcal{L}_{\text{bal}}(\theta) \leq \mathcal{L}_{\text{task}}(\theta) + \frac{1}{2} (\mathcal{L}_H(\theta) - \mathcal{L}_H(\theta_H^*)) + \frac{1}{2} \mathcal{L}_H(\theta_H^*). \quad (65)$$

We now bound the term $\frac{1}{2} (\mathcal{L}_H(\theta) - \mathcal{L}_H(\theta_H^*))$ in the two cases of the theorem.

Parameter route. Assume $\beta \geq \beta_{\min}$ and use Eq. 7 and Eq. 8. For all $\theta \in \mathcal{N}$,

$$\mathcal{L}_H(\theta) - \mathcal{L}_H(\theta_H^*) \leq \frac{L_H^{\text{sm}}}{2} \|\theta - \theta_H^*\|^2 \quad (66)$$

$$\leq \frac{L_H^{\text{sm}}}{2} \frac{2}{m_\Psi} D_\Psi(\theta, \theta_H^*) \quad (67)$$

$$\leq \frac{L_H^{\text{sm}}}{m_\Psi} D_\Psi(\theta, \theta_H^*), \quad (68)$$

where the second inequality uses $\|\theta - \theta_H^*\|^2 \leq \frac{2}{m_\Psi} D_\Psi(\theta, \theta_H^*)$ from Eq. 8. Multiplying by $\frac{1}{2}$ yields

$$\frac{1}{2} (\mathcal{L}_H(\theta) - \mathcal{L}_H(\theta_H^*)) \leq \frac{L_H^{\text{sm}}}{2m_\Psi} D_\Psi(\theta, \theta_H^*). \quad (69)$$

Since $\beta \geq \beta_{\min} = L_H^{\text{sm}}/(2m_\Psi)$, we deduce

$$\frac{1}{2} (\mathcal{L}_H(\theta) - \mathcal{L}_H(\theta_H^*)) \leq \beta D_\Psi(\theta, \theta_H^*). \quad (70)$$

Substituting Eq. 70 into Eq. 65 gives

$$\mathcal{L}_{\text{bal}}(\theta) \leq \mathcal{L}_{\text{task}}(\theta) + \beta D_\Psi(\theta, \theta_H^*) + \frac{1}{2} \mathcal{L}_H(\theta_H^*). \quad (71)$$

By definition,

$$\mathcal{L}_{\text{CL}}(\theta) = \mathcal{L}_{\text{task}}(\theta) + \alpha D_\Phi(h_\theta(\cdot), z) + \beta D_\Psi(\theta, \theta_H^*) \geq \mathcal{L}_{\text{task}}(\theta) + \beta D_\Psi(\theta, \theta_H^*),$$

since $\alpha D_\Phi \geq 0$. Combining this with Eq. 71 yields

$$\mathcal{L}_{\text{bal}}(\theta) \leq \mathcal{L}_{\text{CL}}(\theta) + \frac{1}{2} \mathcal{L}_H(\theta_H^*), \quad (72)$$

, which is Eq. 10 in the parameter route.

Table A1: Implementation details of the considered algorithms for the LTR benchmark.

Algorithm	LR	Opt.	Momentum	LR Scheduler	CL Loss Weight	Epochs	Steps
LwF	0.001	SGD	0.9	–	0.01	5	2
EWC	0.01	SGD	0.9	–	10	90	2
Modified EWC	0.01	SGD	0.9	–	1000	90	2
GPM	0.001	SGD	0	Cosine Anneal LR	–	100	2
SGP	0.001	SGD	0	Cosine Anneal LR	–	150	2
FOSTER (phase 1)	0.1	SGD	0.9	Cosine Anneal LR	–	170	4
FOSTER (phase 2)	0.1	SGD	0	Cosine Anneal LR	–	130	4
TPL	0.01	SGD	0.8	Cosine Anneal LR	–	50	4

Output route. Assume $\alpha \geq \alpha_{\min}$ and use Eq. 9. For all $\theta \in \mathcal{N}$,

$$\mathcal{L}_H(\theta) - \mathcal{L}_H(\theta_H^*) \leq c_\Phi D_\Phi(h_\theta(\cdot), z_H^*). \quad (73)$$

Multiplying by $\frac{1}{2}$ gives

$$\frac{1}{2}(\mathcal{L}_H(\theta) - \mathcal{L}_H(\theta_H^*)) \leq \frac{c_\Phi}{2} D_\Phi(h_\theta(\cdot), z_H^*). \quad (74)$$

Since $\alpha \geq \alpha_{\min} = c_\Phi/2$, we have

$$\frac{1}{2}(\mathcal{L}_H(\theta) - \mathcal{L}_H(\theta_H^*)) \leq \alpha D_\Phi(h_\theta(\cdot), z_H^*). \quad (75)$$

Substituting Eq. 75 into Eq. 65 yields

$$\mathcal{L}_{\text{bal}}(\theta) \leq \mathcal{L}_{\text{task}}(\theta) + \alpha D_\Phi(h_\theta(\cdot), z_H^*) + \frac{1}{2}\mathcal{L}_H(\theta_H^*). \quad (76)$$

Again,

$$\mathcal{L}_{\text{CL}}(\theta) = \mathcal{L}_{\text{task}}(\theta) + \alpha D_\Phi(h_\theta(\cdot), z) + \beta D_\Psi(\theta, \theta_H^*) \geq \mathcal{L}_{\text{task}}(\theta) + \alpha D_\Phi(h_\theta(\cdot), z_H^*),$$

so Eq. 76 implies

$$\mathcal{L}_{\text{bal}}(\theta) \leq \mathcal{L}_{\text{CL}}(\theta) + \frac{1}{2}\mathcal{L}_H(\theta_H^*), \quad (77)$$

which is again Eq. 10, now for the output route.

Combining Eq. 72 and Eq. 77 shows that if either $\beta \geq \beta_{\min}$ or $\alpha \geq \alpha_{\min}$, then for all $\theta \in \mathcal{N}$,

$$\mathcal{L}_{\text{bal}}(\theta) \leq \mathcal{L}_{\text{CL}}(\theta) + \frac{1}{2}\mathcal{L}_H(\theta_H^*), \quad (78)$$

which completes the proof. \square

B.6 Stronger Statement (Special Case): Exact Minimizer Equivalence

For completeness, we recall a special case (useful for exposition) where CL *exactly* optimizes the balanced objective.

Proposition B.2 (Exact equality up to a constant). *Let $\Psi = \mathcal{L}_H$ and assume \mathcal{L}_H is convex on \mathcal{N} . Set $\alpha = 0$, $\beta = \frac{1}{2}$, $\mathcal{L}_{\text{task}} = \frac{1}{2}\mathcal{L}_T$, and z arbitrary. Then*

$$\mathcal{L}_{\text{CL}}(\theta) = \frac{1}{2}\mathcal{L}_T(\theta) + \frac{1}{2}D_{\mathcal{L}_H}(\theta, \theta_H^*) = \mathcal{L}_{\text{bal}}(\theta) - \frac{1}{2}\mathcal{L}_H(\theta_H^*),$$

so \mathcal{L}_{CL} and \mathcal{L}_{bal} have identical gradients and the same minimizers.

Proof. Since $\nabla \mathcal{L}_H(\theta_H^*) = 0$, $D_{\mathcal{L}_H}(\theta, \theta_H^*) = \mathcal{L}_H(\theta) - \mathcal{L}_H(\theta_H^*)$. Add and subtract $\frac{1}{2}\mathcal{L}_H(\theta_H^*)$ and regroup terms. \square

C Implementation Details

All our experiments were conducted using the PyTorch framework. We use the original implementations and training protocols of Learning without Forgetting (LwF), Elastic Weight Consolidation (EWC), a modified version of EWC, Gradient Projection Memory (GPM), Scaled Gradient Projection (SGP), FOSTER, and TPL.¹ The specifics of each

¹The code for the algorithms was obtained and modified from various open-source repositories.

<https://github.com/ngailapdi/LWF>

<https://github.com/shivamsaboo17/Overcoming-Catastrophic-forgetting-in-Neural-Networks>

<https://github.com/MahdiyarMM/Continual-pedestrian-detection>

<https://github.com/sahagobinda/GPM>

<https://github.com/sahagobinda/SGP>

<https://github.com/G-U-N/ECCV22-FOSTER>

<https://github.com/linhaowei1/TPL>

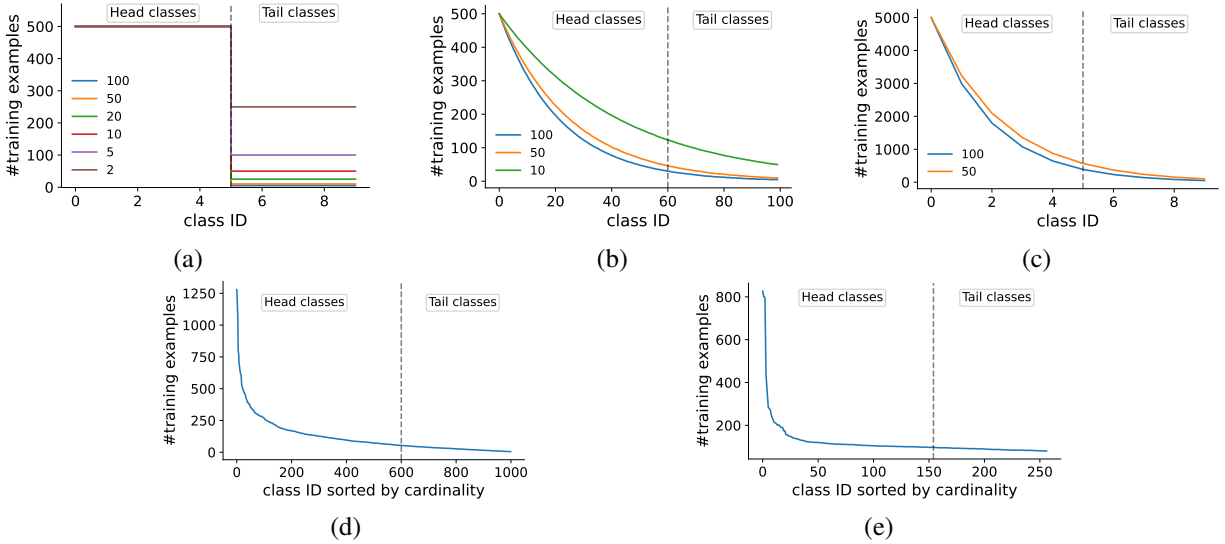


Figure A1: Class cardinality of (a) MNIST-LT, (b) CIFAR100-LT, (c) CIFAR10-LT, (d) ImageNet-LT, and (e) Caltech256.

algorithm’s implementation are summarized in Table A1. The parameters for each algorithm, such as learning rate (LR), optimizer, momentum, LR scheduler, CL loss weight, number of epochs, and number of steps, are detailed there. We mainly follow the original hyperparameter settings recommended for each method, including their training schedules (e.g., number of epochs), and only deviate when strictly necessary (e.g., for algorithm-specific grid search), in order to ensure fair and faithful comparisons.

Note that for SGP, the algorithm-specific hyperparameters are obtained through grid search as follows: $gpm_{\text{eps}} = 0.96$ and $gpm_{\text{eps-inc}} = 0.004$.

D Datasets

Fig. A1 illustrates the distribution of samples among different classes and the division of the dataset into the Head and Tail sections. In the case of CIFAR100-LT with $IF = 100$, the initial partition is configured such that 5% of the samples fall within the Tail and 95% in the Head section (Classes 60 to 100 are classified as Tail). For comparison purposes, the rest of the datasets follow a similar partition threshold where 60% of the classes are assigned to the Head section.

E Algorithm

Algorithm A1 CLTR

- 1: **Input:** long-tailed dataset \mathcal{D} , initialized model parameters θ_i , number of partitions N
 - 2: **Output:** θ_{HT}^*
 - 3: sort \mathcal{D} in descending order by cardinality of each class $|\mathcal{D}_i| \geq |\mathcal{D}_j|$ for all $i < j$
 - 4: partition \mathcal{D} into N subsets \mathcal{D}^i for $i \in [1, N]$
 - 5: sort partitions based on size as $\mathcal{D}^i \gg \mathcal{D}^j$ for all $i < j$
 - 6: initialize CL replay memory \mathcal{M}
 - 7: **for** $t = 1$ **to** N **do**
 - 8: $\theta_t^* = \arg \min \mathcal{L}_{CLTR}(\theta, \mathcal{D}^t, \mathcal{M})$ # CL training
 - 9: update \mathcal{M}
 - 10: **end for**
 - 11: $\theta_{HT}^* = \theta_N^*$
 - 12: **return** θ_{HT}^*
-

F Additional Discussions

F.1 Long-Tailed Class-Incremental Learning

Few prior works have attempted to address the problem of class-incremental learning when the data is heavily imbalanced. A novel replay method called Partitioning Reservoir Sampling (PRS) is proposed in [83]. This method dedicates a sufficient amount of memory to Tail classes in order to avoid catastrophic forgetting in minority classes. In [84], this problem is addressed in two different setups, ordered and shuffled. In the ordered scenario the number of samples in each new task is less than in previous tasks, while in the shuffled scenario, the size of classes is completely random. They propose a two-stage learning method utilizing a learnable weight scaling layer for reducing the bias due to data imbalance. Finally, in [85], OLTR++ is proposed which is a unified algorithm that integrates imbalanced classification, few-shot learning, open-set recognition, and active learning through dynamic meta-embedding and memory association. Note that none of the above works attempt to employ CL as a solution for LTR scenarios.

Here, we compare the performance of CLTR in addressing the LT-CIL problem with the prior state-of-the-art solutions in the area. Following the experimental setup in [84, 86, 87], the models are first trained on the largest 50 classes (Head), then, the remaining classes are learned incrementally in 5 or 10 consecutive tasks (Tail) with an equal number of new classes in each new task, from the largest subset to the smallest subset of the dataset. We apply our method in this setting on the CIFAR100-LT dataset and compare its performance with the prior works, as presented in Table A2. The results demonstrate that CLTR outperforms prior methods in both 5- and 10-task settings by considerable margins of 2.5% and 1.6%, respectively.

Table A2: The performance of CLTR on Ordered LT-CIL Benchmark for CIFAR100-LT

Method	Tasks	
	5	10
EEIL [88]	38.5	37.5
EEIL+2sLWS [84]	39.0	37.6
LUCIR [86]	42.7	42.2
PODNET [87]	44.1	44.0
PODNET+2sLWS [84]	44.4	44.4
LUCIR+2sLWS [84]	45.9	45.7
CLTR (TPL)	48.4	47.3

F.2 Naturally Skewed Dataset

In LTR benchmarks, datasets are modified to exhibit a skewed distribution of samples among various classes. However, such imbalanced class distributions are naturally observed in real-world data as well [5]. To evaluate the efficacy of CL techniques on non-LTR benchmark datasets, we utilize the Caltech256 dataset [54], which consists of 256 distinct classes representing everyday objects. The largest class comprises 827 samples, while the smallest class contains only 80 samples, exhibiting an IF of over 10. Here, we employ the CLTR and compare its performance to the state-of-the-art methods on this dataset for object classification. The results are presented in Table A3. We observe that CLTR outperforms the previous method on this dataset, demonstrating the strong potential of using CL in dealing with long-tailed real-world datasets.

F.3 Practical estimation of β_{\min} and α_{\min}

To illustrate that the conditions in Theorem 3.10 are mild and typically satisfied by standard CL methods, we provide a concrete empirical estimation of β_{\min} and α_{\min} in a real-world setting. We consider a ResNet-18 trained on the Head classes of CIFAR-100-LT, matching our experimental setup.

Estimating β_{\min} : Recall that $\beta_{\min} = \frac{L_H^{\text{sm}}}{2m_\Psi}$, where L_H^{sm} is the local smoothness constant of the Head loss and m_Ψ is the strong-convexity parameter of the parameter-space divergence D_Ψ . We approximate L_H^{sm} by the top eigenvalue of the Hessian of L_H at θ_H^* using Hessian-vector products and power iteration. For the trained ResNet-18, we obtain $L_H^{\text{sm}} \approx 0.2$. When D_Ψ is the standard ℓ_2 divergence (the default choice in many EWC-style methods), the corresponding Bregman divergence is 2-strongly convex, implying $m_\Psi \approx 1$. This gives the practical threshold $\beta_{\min} \approx \frac{0.2}{2} = 0.1$. This value is substantially *below* the regularization strengths typically used in off-the-shelf CL methods (e.g., $\beta = 10\text{--}10^3$ in EWC variants), indicating that the theoretical requirement is easily satisfied in practice.

Table A3: The performance of CLTR on Caltech256.

Method	Backbone	
	Inc.V4	Res.101
$L^2 - FE$ [89]	84.1	85.3
L^2 [89]	85.8	87.2
$L^2 - SP$ [89]	85.3	87.2
DELTA [89]	<u>86.8</u>	<u>88.7</u>
GBN [90]	-	86.9
TransTailor [90]	-	87.3
CLTR (SGP)	88.6	89.8

Estimating α_{\min} : In the unified CL formulation, the output-space regularizer takes the form $\alpha D_{\Phi}(h_{\theta}, z_H^*)$, where D_{Φ} is a Bregman divergence in logit space. In Theorem 3.10, α_{\min} is defined as $\alpha_{\min} = \frac{c_{\Phi}}{2}$, where c_{Φ} is the smallest constant satisfying $L_H(\theta) - L_H(\theta_H^*) \leq c_{\Phi} D_{\Phi}(h_{\theta}, z_H^*)$ for all θ in a local neighborhood. For Bregman divergences D_{Φ} induced by a strongly convex potential in logit space (e.g., squared-logit or KL divergences), this inequality is equivalent to a standard smoothness–strong-convexity relation in the logit domain. In particular, if L_H is L_{out} -smooth with respect to logits and D_{Φ} is m_{Φ} -strongly convex, then $c_{\Phi} = \frac{L_{\text{out}}}{m_{\Phi}}$. Substituting this expression into $\alpha_{\min} = c_{\Phi}/2$ yields the empirically estimable form $\alpha_{\min} = \frac{L_{\text{out}}}{2m_{\Phi}}$, which we use below. L_{out} quantifies the local smoothness of L_H with respect to logits and m_{Φ} is the strong-convexity constant of D_{Φ} . To estimate L_{out} , we compute the largest eigenvalue of the logit-space Hessian $\nabla_z^2 L_H$ at θ_H^* , again using power iteration on batches of Head samples. Since L_H is a batch-averaged loss in our theory, this batch-averaged Hessian is the correct object to analyze. In our ResNet-18 / CIFAR-100-LT Head-class setting, we observe $L_{\text{out}} \approx 2 \times 10^{-4}$. For squared-logit or KL-based output divergences, the associated Bregman divergence is 1-strongly convex in the relevant output domain, giving $m_{\Phi} \approx 1$. Hence, $\alpha_{\min} \approx \frac{2 \times 10^{-4}}{2} = 10^{-4}$. Again, this threshold is far smaller than the regularization strengths commonly used in output-regularized CL methods (e.g., LwF typically uses α between 10^{-2} and 1). Thus, even modest output-space regularization comfortably exceeds α_{\min} .

Both estimated thresholds, $\beta_{\min} \approx 0.1$ and $\alpha_{\min} \approx 10^{-4}$, lie *orders of magnitude below* the α and β values routinely used in practical CL methods. This empirical check supports the conclusion that the theoretical conditions of Theorem 3.10 are not restrictive and are naturally satisfied by off-the-shelf continual learning algorithms.

F.4 Multiple Incremental Steps

Recall that Theorem 3.7 highlights CLTR’s capability for extending beyond two incremental steps. Increasing the number of partitions leads to smaller IF within each partition at the cost of an increase in forgetting. To explore the effect of varying partition numbers on CLTR’s final performance, we adhere to the experimental protocol outlined in [84]. Initially, the model is trained on the first 60 classes, followed by sequential learning of the remaining classes, divided into different numbers of partitions. The results of this experiment are presented in Fig. A2 (left). Our results reveal an optimal value for CLTR (FOSTER) (4 steps), yet the performance margin remains slim even with up to 30 tasks. This highlights the effectiveness of CL methods employed within CLTR. The optimal value for the number of incremental steps for each CL algorithm can be found in Appendix C.

F.5 Replay Memory

Several CL algorithms incorporate mechanisms to retain partial information from the previous task, aiming to mitigate catastrophic forgetting. For example, EWC maintains prior model parameters along with their Fisher values, whereas both GPM and SGP safeguard the Core Gradient Space of previous tasks. FOSTER, on the other hand, utilizes a replay memory for this purpose. Within the LTR context, the presence of a buffer memory doesn’t require additional storage, as access to the full dataset is already available. Nonetheless, to prevent hindering the model’s capacity to learn Tail distributions, we deliberately avoid replaying all Head samples when learning the Tail (evidenced by Eq. 15). Accordingly, our analysis extends to how the number of Head samples replayed while learning the Tail impacts the model’s performance, as illustrated in Fig. A2 (right). The replay memory’s size serves as a mediator between forgetting previous information and worsening class imbalance, e.g. a larger replay memory reduces forgetting but increases imbalance. Therefore, identifying an optimal balance in this trade-off is crucial. Our results demonstrate the

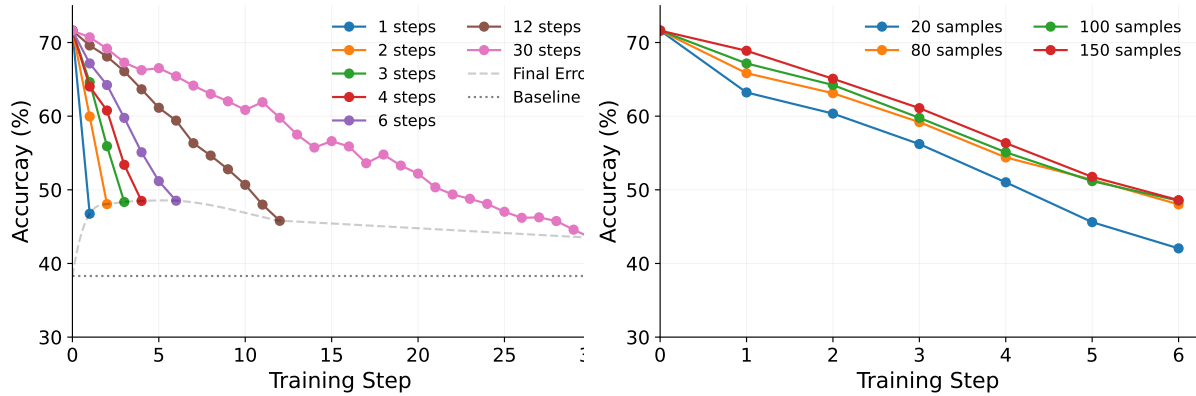


Figure A2: CLTR performance for various (left) number of incremental steps and (right) replay memory (\mathcal{M}) size.

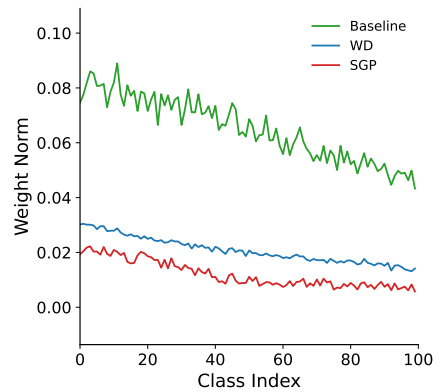


Figure A3: Per-class weight norms of the baseline, SGP, and WD.

significance of an appropriate replay memory size; however, there exists a threshold beyond which additional samples per class do not further improve the performance and the performance levels off.

F.6 Runtime

The inference runtime is identical between CLTR and LTR solutions, due to identical backbones in both types of methods and the fact that CL does not affect inference. Regarding the training runtime, when CLTR is used, the data is divided into Head and Tail sets. At each step of the training, only one partition of data is involved, alongside a replay memory with a limited size. Since the backbone is consistent among all LTR approaches for each benchmark, the runtime is determined by the amount of data fed to the model. Dividing the learning into multiple steps and using CL therefore does not impact the total runtime, nor does it increase the training time significantly.

F.7 Weight Imbalance

An interesting phenomenon observed when training models on highly imbalanced data is the presence of artificially large weights in neurons corresponding to the Head classes [5]. The LTR solution, WD, addresses this problem by penalizing weight growth using weight decay. One way to assess the network’s ability to handle LTR is by analyzing the bias in per-class weight norms. To this end, we present the per-class weight norms of the Baseline, WD, and CLTR (SGP) models in Fig. A3.

The figure reveals a significant imbalance in the weight norms of the Baseline model, which is naively trained on the imbalanced dataset. In contrast, the WD and CLTR (SGP) models exhibit more uniform weight norms across different classes. Interestingly, although CLTR (SGP) starts with the heavily imbalanced weights of the Baseline model, it converges towards a more uniform weight distribution without any explicit penalty on weight growth. Unlike many other CL methods that restrict the plasticity of crucial weights, SGP only constrains the direction of the weight update

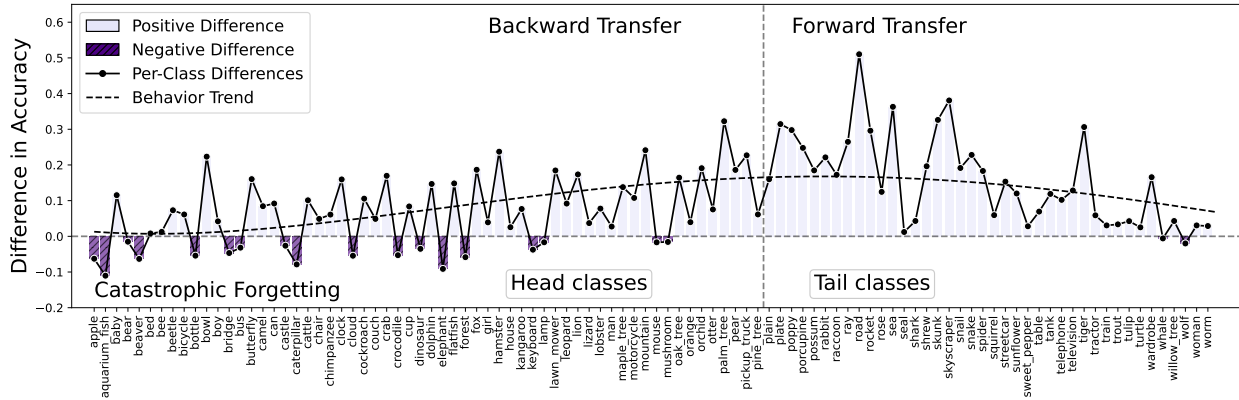


Figure A4: The difference in per-class accuracy of CLTR (SGP) and the baseline model. 

in the weight space, enabling the model to converge to a more balanced weight distribution. This further demonstrates the effectiveness of CL in addressing LTR problem.

E.8 Backward/Forward Transfer and Catastrophic Forgetting

Prior works discuss three key concepts in the context of CL: catastrophic forgetting, backward transfer, and forward transfer [65]. As mentioned earlier, catastrophic forgetting occurs when the performance of a class declines after retraining. Despite the use of CL methods, which are designed to mitigate this forgetting, a certain degree of forgetting is still inevitable. Forward transfer is the improvement in performance on a new task after employing CL, which is the central aim of retraining in CL. Finally, backward transfer is a beneficial side-effect where retraining on new samples can actually enhance the model’s performance on the previous tasks. This interesting phenomenon in CL has been extensively discussed in previous works in theory and practice [91]. Now, let’s discuss Fig. A4, which presents the difference in per-class accuracy of CLTR (SGP) versus the baseline network. The analysis is based on CIFAR100-LT with an IF of 100. The figure is divided into three regions corresponding to the scenarios discussed above: catastrophic forgetting (bottom), backward transfer (top-left), and forward transfer (top-right). The bottom region in the figure represents classes that undergo catastrophic forgetting, while the top-right region represents the Tail samples (with a class index larger than 60), which demonstrate improved performance, or forward transfer. We observe that using SGP as a CL solution for LTR results in very effective improvements in the per-class accuracy of the Tail (forward transfer). Interestingly, despite the absence of Head data in the retraining process, 42 out of 60 Head classes see some level of improvement after the model is exposed to the Tail samples (backward transfer). This result emphasizes the remarkable potential of CL methods in enhancing performance in both new and previous tasks.